CHARACTERIZATION AND QUANTIFICATION OF FOREST SECONDARY STRUCTURE USING AIRBORNE LIDAR

by

Lukas Ryan Jarron
B.Sc., The University of British Columbia, 2017

A THESIS SUBMITTED IN PARTIAL FULFILLMENT OF
THE REQUIREMENTS FOR THE DEGREE OF

MASTER OF SCIENCE
in
THE FACULTY OF GRADUATE AND POSTDOCTORAL STUDIES
(Forestry)

THE UNIVERSITY OF BRITISH COLUMBIA
(Vancouver)

August 2020

The following individuals certify that they have read, and recommend to the Faculty of Graduate and Postdoctoral Studies for acceptance, a thesis entitled:

Characterization and quantification of forest secondary structure using airborne LiDAR

submitted by Lukas Ryan Jarron in partial fulfillment of the requirements for

the degree of Master of Science

in Forestry

Examining Committee:

Dr. Nicholas C. Coops, Professor, Department of Forest Resource Management
Supervisor

Dr. Suzanne Simard, Professor, Department of Forest and Conservation Science
Supervisory Committee Member

Mr. William H. MacKenzie, Provincial Research Ecologist, Government of B.C. - FLNRO
Supervisory Committee Member

Dr. Cindy Prescott, Professor, Department of Forest and Conservation Science
Additional Examiner

Abstract

Knowledge of forest structure can be used to guide sustainable forest management decisions. Currently, Airborne Laser Scanning (ALS) has been well established as an effective tool to delineate and characterize canopy structure of forested biomes. However, the use of ALS to characterize forest secondary structure is less well developed. Secondary structure consists of suppressed sub-canopy trees, short-stature vegetation and coarse-woody-debris (CWD). I utilized discrete return ALS to develop methodologies which characterize two of these secondary structural units, sub-canopy trees and CWD, within natural forest stands in central British Columbia. I first segmented the forest vertically into canopy versus sub-canopy and computed a suite of ALS metrics to develop predictive models of sub-canopy stand attributes. Calibrated against 28 ground plots, models were developed using stepwise regression resulting in the strongest predictors being a combination of height, structure and cover-based metrics. Two sets of models were developed, one with the canopy removed and another with it retained. The sub-canopy set of models resulted in stronger cross-validated R-squared values for volume and basal area and as a result the sub-canopy volume model was used to map sub-canopy volume over the entire study area. The second structural unit, CWD, is a meaningful contributor to forest carbon levels and biodiversity. In this work I detail a novel methodology that isolates CWD returns from large diameter logs (>30cm) using a refined grounding algorithm, a mixture of height and pulse-based filters and linear pattern recognition to transform returns into measurable vectorized shapes. Height values are extracted directly from the point cloud to calculate volume for detected shapes. This approach is then demonstrated by successfully mapping CWD and estimates of volume as well as providing an assessment of individual log and plot-level attributes that influence successful detection. I compared plot volume totals calculated from ALS-derived

CWD against field measured CWD and found a strong correlation. Lastly this methodology was applied over a larger region to quantify CWD volume differentials between stands. These methodologies demonstrate the capability to generate a secondary structure inventory that can highlight locations for selective logging, model fire susceptibility and carbon sequestration, and quantify wildlife habitat.

Lay summary

Forest structure provides valuable insight into the productivity of the world's forests by influencing habitat, temperature and resource availability. To properly prepare our forests for the future, a detailed knowledge of their structural arrangement is required. Airborne laser scanning is a technology that can be flown over large areas and produce a three-dimensional representation of structure. This technique is commonly used to assess the forest canopy however, much of the structure beneath the canopy is often overlooked. This research focus on using airborne laser scanning to measure two specific units beneath the canopy, sub-canopy trees and fallen logs. A novel method to measure sub-canopy trees is developed and displays the ability to estimate volume of these trees. A separate method is then developed to map and quantify log volume. The products of this research can be used to update forest inventories and provide insight on where to optimally locate forest resources.

Preface

My supervisory committee members, along with Ms. Pamela Dykstra, all aided in the framing of my research questions and provided suggestions, edits and feedback. These research questions have been developed into two scientist papers and are the core of this thesis. With guidance and input from Dr. Nicholas Coops, I was responsible for defining the methodologies, processing and analysing the data, interpretation and presentation of the results and the production and refinement of the manuscripts. Mr. William Mackenzie developed the concept of the percentage-based variable canopy threshold outlined in Chapter 3 and helped provide the ALS data. Dr. Piotr Tomplaski provided technical advice and guided software implementation for Chapter 3 and provided editing and feedback throughout, as such he has been listed as a co-author for Chapter 3. Dr. Suzanne Simard provided helpful insight into the focus and implications of Chapter 4. All committee members edited and proofread each chapter of this thesis. The research presented in this thesis has been published or is under review for publication as listed below.

Chapter 3: Jarron, L.R., N.C. Coops, W.H. MacKenzie, P. Tompalski and P. Dykstra. 2020. Detection of sub-canopy forest structure using airborne LiDAR. Remote Sensing of Environment. 244, 111770.

Chapter 4: Jarron, L.R., N.C. Coops, W.H. MacKenzie, and P. Dykstra. 2020. Detection of sub-canopy forest structure using airborne LiDAR. (Under review)

Work contained in this thesis has also been presented as:

Jarron, L.R., N.C. Coops, W.H. MacKenzie, P. Tompalski and P. Dykstra. Detection of sub-canopy forest structure using airborne LiDAR. Poster presented at the 16th Silvilaser Conference; 2019 Oct 8-10; Iguazu Falls, Brazil.

Table of Contents

List of Tables

List of Figures

List of Abbreviations

ABA – Area based approach

ALS – Airborne laser scanning

BA – Basal Area

BA_{SC} – Sub-canopy basal area

BGC – Biogeoclimatic

CI – Confidence interval

CoV – Coefficient of variation

CSF – Cloth simulation filter

CWD – Coarse-woody debris

DBH – Diameter at breast height

ESSF – Engelmann spruce sub-alpine fir

HL – Lorey's mean height

LAD – Leaf area density

LiDAR – Light detection and ranging

N_{SC} – Number of sub-canopy trees

NDVI – Normalized difference vegetation index

P95 – 95^{th} height percentile

SBS – Sub-boreal Spruce

SPL – Spaceborne laser scanning

TLS – Terrestrial laser scanning

V_{SC} – Sub-canopy volume

VRI – Vegetation resource inventory

Acknowledgements

I would like to thank the BC Ministry of Forests, Lands, Natural Resource Operations and Rural Development for their funding and commitment to advancing research as well as BC Timber Sales for providing the ALS data. Thank you to everyone involved in the PEM research group for your support and ideas. Specifically, I would like to thank Colin Chisholm for his valuable insight and collaboration as well as Pamela Dykstra for framing the work and providing the infrastructure to make it possible. Agatha, Marco and George, thank you for your hard work in the field and bearing with me through the sweat, dead-ends roads, and bee stings. Piotr and Tristan, I am grateful for your technical guidance and for answering all my coding questions.

To my supervisory committee, thank you for taking the time out of your busy schedules to consistently provide me feedback that has really helped refine the final product. Will and Suzanne, your industry and ecological insight has been crucial to keeping the research moving in an applicable direction. A huge thank you to Dr. Nicholas Coops for your constant support, guidance and belief in me since taking me on as an undergrad research assistant five years ago, right through to the fruition of this thesis. You sparked and encouraged my interest in remote sensing and for that I will always be grateful. To all members of the Integrated Remote Sensing Studio, working alongside you as been both inspiring and gratifying. I would like to express my appreciation for the support, kindness and good times you have shown me over the past years.

I would also like to extend thanks to my godfather Len for introducing me to forestry in B.C., my long-time roommates John and Evan along with the UBC track community for their ongoing support and encouragement. Lastly to my family, thank you for always being there for me and for your unwavering support in every sense of the word.

Dedication

I dedicate this thesis to my late dog Finnegan. You were a perpetual source of stability and unconditional love who taught me to appreciate myself, others and the world in a way no human ever could. Love you buddy 🐾

Chapter 1: Introduction

1.1. Introduction

Forested landscapes are dynamic, and multi-faceted ecosystems that dominate more than one-third of the Canadian landscape (Natural Resources Canada, 2018). Across Canada, forests vary in height, density and composition largely due to climatic variables however, due to resource limitations and geopolitical boundaries, local scales are where forest management decisions most often take place and where a deeper understanding of forest structure is required to guide the decision making process (Bunnell and Boyland, 2003; Shifley et al., 2017). In place of climatic variables, forest diversity at the local scale, along with the ecosystems they encompass, are more influenced by the surrounding environment and the biophysical structure of the forest stand (Bohn and Huth, 2017). In the northern coniferous forest of British Columbia, the structural development of forest stands drivelandscape-level processes and reflect many stand-level factors such as temperature regimes, site condition, species composition, successional stage and past disturbances, all of which are critical aspects of forest ecosystems as habitat for other biota (Franklin et al., 2002; Larson et al., 2005). The cycle between these natural processes creates a variable range of forest structure and composition between stands and across spatial and temporal scales (Landers et al. 1999; Lertzman et al. 1998; Peterson et al. 1998; Peterson 2002; Turner 1989). Knowledge surrounding forest structure can provide insight into the myriad of ecosystem services influenced by forest structure including habitat availability, nutrient cycling and long-term carbon sequestration. As such, accurate representations of forest structure have become a critical component of effective forest ecosystem management (Lefsky et al. 2002; Guo et al., 2017) especially in the northern coniferous forests of British Columbia (Coops et al. 2007).

The structure of forested landscapes, defined as the spatiotemporal variance of forest structural elements (Zhang et al., 2017), is the key driver of stand-level forest dynamics (Spies, 1998) that sustain and influence ecosystems. Productivity of forests, both economically in terms of timber supply (Fantini and Guries, 2007) and ecologically in terms of biodiversity (Bohn and Huth, 2017), can be summarised by the vertical and horizontal distribution the size, density and arrangement of woody biomass. The interactions between structural elements have been highlighted as biodiversity indicators across a multitude of forested ecosystems (Chirici et al., 2011; Gao et al., 2014) and are known to influence the future composition of the forested landscape through nutrient and light availability (Martinuzzi *et al*., 2009; Lochhead and Comeau, 2012), making characterization and classification of forest structure a focal point for forest managers and recent forest research efforts (Wallace et al., 2016; Lelli et al, 2019; Koontz et al., 2020). Specifically, identifying locations with high degrees of structural complexity is important to forest managers as these stands are often the most productive and positively correlated with high levels of species richness (Brunialti et al. 2010; Taboada et al. 2010). Identifying and predicting the physical structures of forest stands is crucial in order to understand the complex interactions of the dynamic systems present within and between stands.

The overall structure of a forest stand is an aggregate of different woody elements including canopy trees, sub-canopy trees, short-stature vegetation, standing dead snags and coarse woody debris (CWD) arranged in an array of sizes, densities and spatial orientations, that make uniform quantification and classification complicated. Instead, separate measurements exist to characterize individual aspects of forest structure. A common classification applied to characterize the temporal aspect of forest structure development in British Columbia is segregating forest stands into successional stages (Horn 1975; Shugart, 1984; Swanson et al.,

2011). Typically, this is related to the age of the forest relative to the most recent disturbance and its intensity, which is noted as being one of the most influential factors driving forest structure (Bolton et al., 2017). Successional stages provide insight into the relative stand age and species associated with that stage. Successional stage is one of many parameters that begin to describe forest structure, however many more such as tree height (Zimble et al., 2003), density (Zheng et al., 2019), leaf-area index (Coops et al., 2007) and volume (Goodbody et al., 2016) have proven useful in obtaining a well-rounded understanding of local forest structure. Combinations of these have also be quantified into structural stage indices and applied to represent the overall complexity of a stand (del Rio et al., 2016; Caviedes and Ibarra, 2017).

While the aforementioned structural measurements are largely representative of horizontal distributions of forest structure, stand structure can also be classified within a stand into vertical strata most commonly into five categories: canopy trees, sub-canopy trees, understory vegetation, standing dead snags and coarse-woody debris (CWD). Undoubtedly the most well-researched of these strata is the canopy (Van Leeuwen et al., 2010; Bolton et al., 2013; Hilker et al., 2013; Hermosilla et al., 2014) as it contains the largest and most economically valuable trees for timber production. Canopy trees also have ecological influence over lower strata as well by facilitating understory development and creating competition for limited resources (Reigel et al., 1992). Due to the explicit economic value and influence of dominant canopy trees the attributes and structural patterns associated with the forest canopy have been well documented and inventoried, however forested ecosystems are integrated entities consisting of much more than just the canopy (Franklin *et al*. 2002). Movement towards more detailed inventories that include a greater breath of forest structural components will be vital to managing British Columbia's forests.

1.2. Forest secondary structure

Forest secondary structure excludes the primary structure of the canopy and consists of the three remaining vertical strata including sub-canopy trees, understory vegetation, and deadwood, both standing snags and coarse-woody debris (CWD) (Connell et al., 1997). The development and composition of secondary forest structure is a key characteristic of forest succession dynamics (Nilsson and Wardle, 2005) and therefore is critical for predicting future forest structure in order to implement the appropriate management decision for each stand. In the northern coniferous forests of British Columbia, a simplified trajectory of forest development after stand-replacing disturbance will include several phases: establishment of a new trees, stem exclusion and canopy stratification of the initial even-aged cohort of young trees; establishment of shade-tolerant understory species; mortality of individuals and gap dynamics leading to the replacement of the initial cohort by the shade-tolerant cohort through mortality creating a complex multi-aged canopy structure. The later stages are defined by heights, densities and shade-tolerance of trees beneath the canopy (Province of British Columbia, 2015).

The presence and characteristics of the forest sub-canopy influences functions in forest ecosystems through changes over time in the architecture of wildlife habitat, resulting in forage and shelter from predators (Nijland *et al*., 2014). Vertical stratification in the sub-canopy also determines fuel loading and presence of ladder fuels. The understory composition predicts wildfire intensity and the likelihood of surface fires spreading to crown fires. (Keane 2014), which are becoming more frequent in Western North America. Canopy species composition is also strongly influenced by sub-canopy conditions through gap dynamics (Yamamoto, 2000; Muscolo *et al*., 2014), which influence local timber supply. The sub-canopy portion of the forest

stand also represents a substantial component of species diversity in British Columbia (Coates *et al*., 2012).

Characterization and a quantifiable inventory of secondary forest structural attributes is vital for making sound forest management decisions in British Columbia that consider all aspects of a forest stand as an integrated system rather than isolating primary structure as a representation of the wider ecosystem. Of the secondary structural units, short-stature understory vegetation is simplest to vertically discern from the canopy and has been the focus a considerable amount of recent research (Campbell et al., 2018; Krebs et al., 2019; Hillman et al., 2019). Alternately, sub-canopy trees which are composed of intermediate sized trees and regenerating saplings, are well recognized for their importance to stand structure and forest succession (Pyke and Zamora, 1982) but have received less attention due to the lack of tools available to remotely observe and quantify them into inventories.

Given the influence of advanced regeneration trees on multiple resource values, increased knowledge of the distribution of sub-canopy regeneration trees can improve integrated forest management. Identification of areas with a well-developed sub-canopy can be used to generate a sub-canopy inventory to guide modern harvesting and silvicultural systems such as partial cutting and shelterwood to manage local timber supply. Used properly, these retention-based silvicultural systems can be used in place of traditional clear cutting to achieve desired management outcomes related to wildfire mitigation, regeneration establishment of climate adapted tree species, carbon sequestration, local timber supply and management of wildlife habitat attributes. Detailed metrics of forest secondary structure can help determine stand successional stage and condition to compare stands diversity across a landscape. As a result, the ability to efficiently measure the structural and spatial arrangements of sub-canopy attributes has

potential as a valuable tool for planning tactical forest management and deploying harvesting and silviculture practices to meet multiple resource objectives in the temperate forests of British Columbia.

Detailed information on sub-canopy structure presents forest managers with opportunities for retention harvest strategies in an era where clearcuts in British Columbia are continually comprising lesser amounts of the total timber harvest on public land (British Columbia Ministry of Forests and Range, 2018). This trend is expected to continue due to public scrutiny around the visual appearance of large clearcuts and to address multiple resource values in integrated forest management. As we continue to approach forest management from an increasingly broader perspective, and under changing natural disturbance regimes, quantifying and mapping of the sub-canopy will aid in gaining a more comprehensive understanding of our forests from both and an ecological and local timber supply perspective.

1.3. Coarse-woody debris

The final category of forest secondary structure is deadwood, either standing snags or residual from fallen trees known as CWD. Individual snags have been detected with ALS by Wing et al. (2015), noting their importance to forest structure through providing habitat and carbon storage. Snags eventually decay and fall to become CWD but maintain their critical role in forest ecosystems. The amount, type and condition of CWD on the forest floor is an important component of the terrestrial carbon cycle and can provide key insights into forest stand history and is greatly impacted by both natural and anthropogenic disturbances. CWD is specifically required to be estimated when reporting under the United Nations Framework Convention on Climate Change, as it is one of the five pools of carbon in terrestrial ecosystems (Kimberley et

al., 2019). CWD represents an important transitional state for carbon stored within a forest stand as it will gradually emit stored carbon as it decays (Malhi et al., 1999; Pan et al., 2011). Latitudinal gradients influence decay rates and result in the CWD of northern forests of British Columbia largely being a carbon sink (Woodall and Liknes, 2008). Decay rates and structure of CWD also varies among species (Harmon et al., 2020) and between disturbed and undisturbed forest (Schmid et al, 2016), with completely undisturbed forest contributing less to the carbon pool and severely disturbed forests often resulting in large quantities of CWD which become the primary substrate for microbial decomposition (Amiro et al., 2010; Russell et al., 2014). This variability of carbon within different states of CWD highlights the need for a direct CWD quantification and mapping procedure to develop reliable landscape-level management models.

In addition to carbon, accumulation and decomposition of CWD are important drivers for local abundance, distribution and composition of forest wildlife (Harmon et al., 1986). CWD in northern coniferous forests are known to store water and essential nutrients (Laiho and Prescott, 2004) that provide ideal microsites for habitat (Harmon and Fraklin, 1989). CWD volume and composition is known to affect habitat quality (McComb, 2003) for insects to large mammals. Primary decomposers who are largely contribute to nutrient cycling in forests, such as beetles and fungi, rely on CWD as an energy source and have been found to be more abundant in areas with greater CWD (Zhou et al., 2007; Sahlin and Ranius, 2009). Small mammals such as the red-backed vole (Ucitel et al., 2003) are reliant on CWD as it provides nesting habitat, thermal shelter and cover from predators (McComb, 2003). In British Columbia, Canada alone, 51 vertebrates are known to be supported by CWD (Kiesker, 2000). Vertebrates tend to select CWD logs with a larger diameter more often as habitat (Rondeux and Sanchez, 2010; Wilbert et al. 2000), as these logs decay at a slower rate and can provide larger nesting cavities. Locating these

large CWD logs would allow forest and wildlife managers to optimize spatial allocation of their resources.

CWD is strongly linked to fuel load estimates for forest fires. Alongside duff/litter and understory vegetation, CWD represents one of the three main elements of the fuel complex (Lutes and Keane, 2006). As such, CWD has been a common measurement taken in studies looking to assess surface fuel loading (Cansler et al., 2019; Choi et al., 2015; Aponte et al., 2014; Rollins et al. 2004). Prescribed burns have also become more commonplace and are kept under control in part by selecting areas with the ideal amount of CWD fuel present. Larger pieces and greater volumes of CWD tend to burn longer and are closely linked with fire effects such as combustion emissions and soil heating (Lutes and Keane, 2006). Quantification of CWD in forest stands would be beneficial for selecting optimal locations for these prescribed burns. Additionally, wildfire severity, extent and frequency have increased in Western North America over the past decade (e.g., Halofsky et al. 2020, Kirchmeier-Young, 2019). With this trend predicted to continue, knowledge of CWD fuel volume and distribution would lead to more efficient wildfire management and potentially a reduction of fire severity and extent and even assist with wildfire mitigation and prevention. Identifying the spatial distribution of CWD volume could assist with wildfire management by allowing forest managers in B.C. to identify areas with high fuel loading and consequently, high fire severity potential.

The development of CWD volume and distribution maps is needed to update a range of forest-related inventories including carbon and wildfire fuel loads estimates. Any forest inventory system requiring carbon estimates would benefit from a quantifiable measurement of CWD as it is one of the main carbon pools required for reporting carbon budgets (Kimberley et al., 2019). Forest and wildlife managers can utilize CWD maps to highlight forested regions containing the

most and least CWD volume. The identification of these areas can provide spatially explicit details on potential habitat location for the multitude of species which rely on CWD. Additionally, fuel load maps describing susceptibility to wildfire would also benefit from a spatial description regarding the distribution of CWD fuel. Lastly, research studies focusing on CWD could utilize these maps to identify areas with the specified amounts of CWD to guide optimal plot selection. As forest management becomes an increasingly critical aspect in the adaptation to a changing climate, understanding of the spatial distribution and quantity of CWD within British Columbia's forests is needed to provide local forest managers with the necessary information to assess, evaluate and manage CWD into the future.

1.4. Remote Sensing of forest structure

Ground-truth data acquisition provides the most accurate description of sub-canopy structure and CWD however, field-based approaches are labour and financially restrictive (Hall, 2005). More recently, knowledge surrounding the structure, diversity and functions of forests has become increasingly detailed with the continued advancements of earth observation and remote sensing technologies allowing for unprecedented large-scale acquisition of forest spatial information (Wulder, 2004). Even the most basic technologies such as aerial photointerpretation have been used to predict simple forest structure and composition with success over large areas (Stone, 1998; Franklin et al., 2001). Satellite imagery, such as the free and open access Landsat archive (Woodcock et al., 2008), has progressed to direct spacebourne modelling of forest structural parameters (Feely et al., 2005; Hall et al., 2006) and disturbances regimes that predate and influence forest structure (Pflugmacher et al., 2012; Hermosilla et al., 2018). Aboveground forest biomass has also been estimated using both optical imagery (Lu, 2005) and RADAR sensors

(Hensley et al., 2013). RADAR application is notably limited based on terrain and soil moisture conditions (Wulder, 1998) while optical sensors are restricted by spatial resolution and specifically a two-dimensional representation of a three-dimension attribute (Lovell et al., 2003), despite impressive spatial range and temporal histories.

Alternatively, light detection and ranging (LiDAR) is an active remote-sensing technology that measures the return times of laser pulses to directly capture three-dimensional information with high spatial resolution and vertical accuracy. This type of data is particularly useful for estimating the vertical variation of biophysical structures such as forest structure across spatial gradients (Dubayah and Drake, 2000). Application of this technology towards forest structural measurements has been demonstrated using a range of different platforms including terrestrial laser scanning, (TLS) (Danson et al., 2007) airborne laser scanning (ALS) (Kim, 2003; Hudak et al., 2008; Guo et al., 2017) and spaceborne laser scanning (SLS) (Qi and Dubayah, 2016; Duncanson et al., 2020). TLS provides an extremely dense and detailed point cloud but has spatial and mobility restrictions influenced by terrain (Liang et al., 2016) while SLS is currently unable to capture an entire forest stand at a uniform density and is better suited for global-scale analysis.

Comparatively, ALS can be conducted from a plane or unmanned aerial vehicle over a specified geographical area providing an optimal balance of spatial extent and resolution to characterize forest stands at the landscape level. Furthermore, ALS has customizable acquisition parameters to cater to the desired density, spatial coverage and cost (White et al., 2013). Advancements in LiDAR technology have resulted in an increasing density of ALS footprints and decreasing acquisition costs. The majority of contemporary and commercially used LiDAR systems produce discrete-return data (Lindberg et al., 2012) which contributes 1-5 returns per pulse and

can penetrate through overstorey canopy providing direct interactions with sub-canopy forest structures. Sub-meter vertical accuracy from discrete return ALS has been reported by multiple sources (e.g., Reutebuch *et al.*, 2003; Schenk, 2001). Specifically, ALS has previously proven effective at measuring forest structural attributes relating to height, biomass, basal area, density and foliage indices (Coops *et al.*, 2007), highlighting the potential to transfer and apply these measurements to a sub-canopy context. CWD characterization also greatly benefits from the recent advancements in the density of ALS technology as historical quantification efforts have relied on indirect modelling based upon other structural attributes (Pesonen et al., 2008; Van Aardt et al., 2011). Alternatively, modern point clouds offer detailed visualizations of the forest floor and associated CWD (Nystrom et al, 2014; Lindberg et al., 2013; Joyce et al., 2019), which presents an opportunity to directly characterize and model this important component of forest structure.

New opportunities now exist to utilize ALS to characterize and inventory secondary structural components in forests stands such as sub-canopy structure and CWD that were previously overlooked by other remote sensing technologies. Using ALS to produce maps detailing the location and quantity of sub-canopy structure and CWD can fill the need for updated biomass estimates along with ecosystem and successional stage classifications for the existing Vegetation resource inventory polygons (VRI), which are currently interpreted primarily from aerial photo interpretation. VRI covers most of British Columbia; VRI could be updated with ALS-derived CWD and sub-canopy structure inventories across the province as provincial ALS coverage continues to increase. Integration of stand-level forest secondary structure characterization using ALS can provide the VRI with the detailed landscape-level inventory required to manage these important forest attributes.

1.5. Research Objective and thesis overview

The objective of this research was to evaluate the ability of ALS to locate and quantify secondary structural attributes within the natural forest stands of central British Columbia. Forest managers could greatly benefit from the spatial identification of these structural elements that influence the anthropogenic and ecological values of their surrounding ecosystems. To address this objective, the investigation was broken down into two specific research questions:

1. Can sub-canopy trees and stand characteristics of naturally regenerating forests be quantified using ALS?

2. Can CWD attributes such as spatial location and volume be accurately mapped and detected from ALS in naturally regenerating forest stands?

Chapter 2 provides detailed information on the study area including climate, topography and dominant vegetative species. Additionally, it outlines the ALS acquisition characteristics as well as the sampling procedure undertaken to obtain a diverse field-based representation of a range of forest structures.

Chapter 3 describes a novel methodology for defining the sub-canopy and separating it from the dominant canopy. This chapter illustrates the application of this methodology to derive predictive models of quantifiable sub-canopy attributes from a suite of ALS metrics that are used to generate a sub-canopy map.

Chapter 4 details a novel processing strategy for spatially isolating CWD returns within the ALS point cloud and transforming them into measurable vectors to generate volume estimates. The methodology is applied to produce CWD volume maps. Accuracy diagnostics are then conducted

at the individual log, plot and stand level to determine characteristics that influence CWD detection rates.

Chapter 5 highlights the key findings and draws conclusions from previous chapters. Limitations are addressed along with recommendations for future research.

Chapter 2 - Study area and design

2.1. Study area

The study area is located between the communities of Smithers and Houston in central British Columbia (54.7°N, 126.9° W). It occupies 48,000 ha of primarily conifer forest of the Deception Lake operating area of BC Timber Sales. Climatically, British Columbia is classified into Biogeoclimatic (BGC) zones that use climax vegetation communities to infer the grouped ecological effects of climate and soil (Mackenzie and Meidinger, 2018). The study area occurs in the Sub-Boreal Spruce moist cold; Babine variant (SBSmc2), and Engelmann Spruce – Subalpine Fir moist cold subzone (ESSFmc) biogeoclimatic units (Banner et al. 1993) (Figure 1). Within both climate areas the dominant tree species are *Abies lasiocarpa* (subalpine fir), *Pinus contorta* (lodgepole pine) and *Picea engelmannii* x glauca ("interior" spruce). *Picea mariana* (black spruce), *Populus tremuloides* (trembling aspen), *Alnus incana* (mountain alder), *Betula papyrifera* (paper birch) and *Salix scouleriana* (Scouler's willow) are found in low densities primarily at lower elevations of the study area. The region is mountainous with elevation ranging from 700 - 1550m and has been actively managed for forestry, resulting in a mosaic of second growth and mature old-growth forest. Within the study area, VRI units have been delineated via photo interpretation representing a variety of stand ages, heights and structures. Ground-level vegetation and shrub density varies with soil moisture and stand successional stage. The mean annual precipitation for the region is 660mm and mean annual temperature ranges from 0.5°C to 3.1°C depending on elevation (Wang *et al*., 2007). Forest fires are also frequent (B.C. Ministry of Forests, 1998).

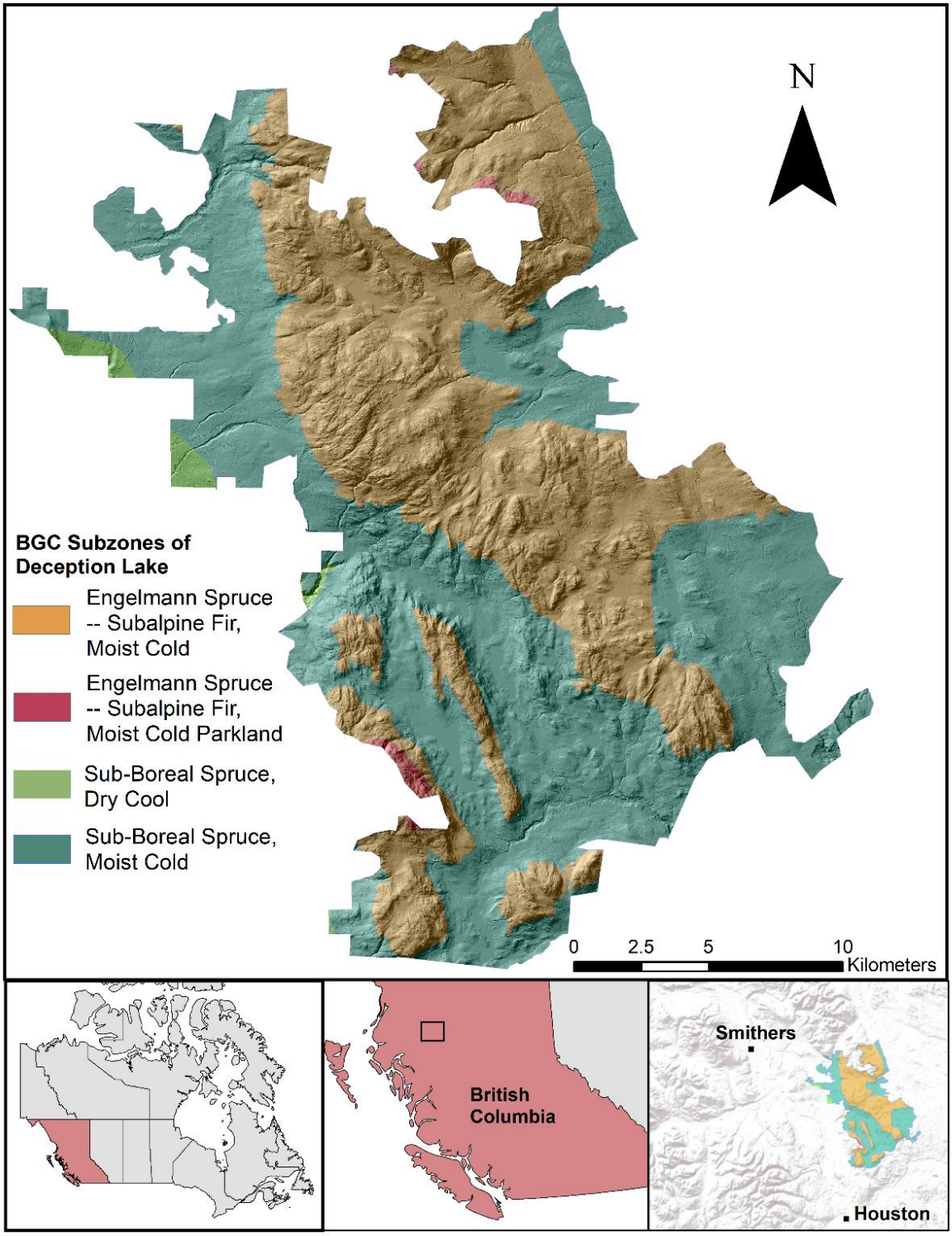

Figure 1. Map of the Deception Lake operating area and associated BGC subzone/variants near Smithers in northwestern British Columbia.

2.2. ALS data and pre-processing

Discrete-return ALS data were acquired over the entire forest management unit over the period of August 6th to 22nd 2016. Collection at this time of year ensured full leaf coverage providing a realistic representation of forest and sub-canopy. This dataset consists of a relatively high point density of 23 points/m^2 (Table 1) and up to a maximum of six returns per pulse. This high density ALS dataset provides unique opportunity to describe structural aspects of forests that are often overlooked by other remote sensing technologies due to the ability to know where, in the vertical forest structure, the reflective surfaces are located (Miller *et al*., 2003). The ALS data was filtered for noise returns and normalized following standard point cloud processing routines within LAStools (Isenburg, 2014), similar to those described in a best practices guide for generating forest inventory attributes from ALS (White *et al*., 2013).

Table 1. ALS acquisition characteristics for Deception Lake, B.C.

Characteristic	2016 LiDAR
Sensor	Riegl Q 1560
Wavelength	1064 nm
Flying altitude	1200m
Flying speed	140 Kts
Scan rate	800 Khz
Scan angle	58°
Minimum overlap	55%
Average point density	23 per m^2
Average pulse density	10 per m^2

2.3. Plot selection

In order to capture the range of forest structure present in the study area a structurally guided sampling approach was used (Nijland *et al*., 2015). Three ALS metrics, gridded at a 20m resolution, were chosen to guide the sampling: 1) normalized average height of the 95th percentile (P95); 2) proportion of normalized returns above 2 meters; and 3) normalized point height coefficient of variation (CoV). These metrics were chosen to guide sampling as they represent the three metric categories that describe forest structure (Coops et al. 2016). P95 represents canopy height, proportion over 2 meters represents canopy cover and CoV represents vertical height distribution. Additionally, the metrics have been individually identified as key variables for describing forest structure (Matasci et al., 2018). Each metric was stratified using equal breaks along their respective ranges into four separate classes to capture the range of these key metrics. (Figure 2). Of the potential 64 unique combinations of the original three ALS metrics, the result was 14 dominant structural classes representing unique forest structure spread over a range of BGC zone variants. Each class was sampled twice for a total of 28 plots. For accessibility purposes, plots were required to be within 250 m of a road.

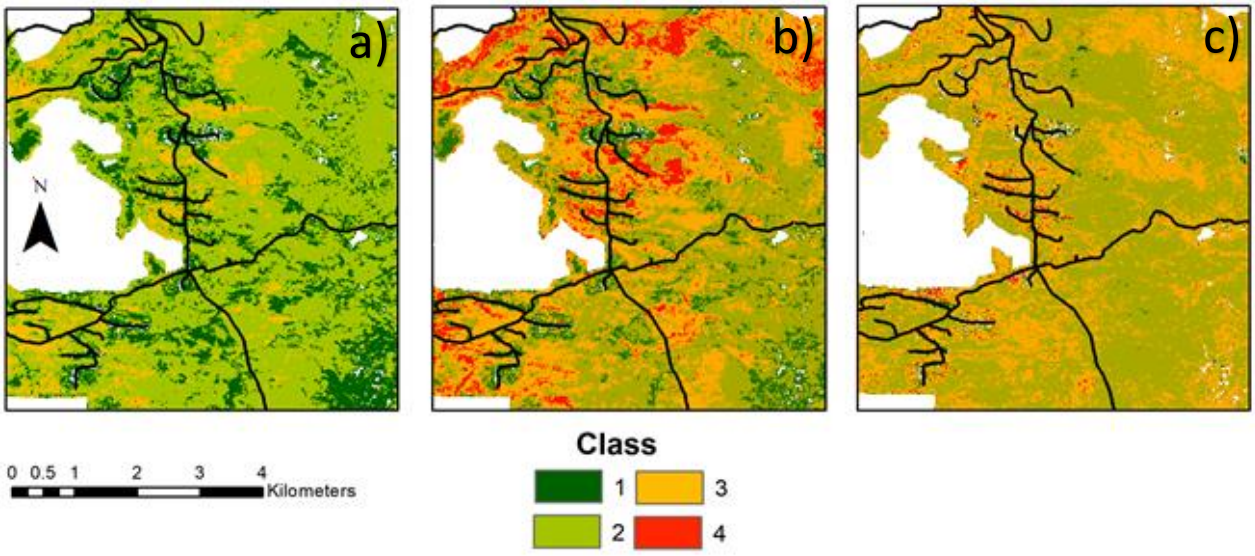

Figure 2. ALS metric-based stratification results for Deception Lake, B.C. Four classes representing proportion of returns above 2 m (a), height of the 95th percentile (b) and coefficient of variation (c).

2.4. Plot measurements

Field work was conducted by a four-person field crew in August, 2018 and focused on two primary sets of measurements, stand inventory and CWD measurements. Following the suggested best practices for describing stand inventory attributes from ALS (White *et al.* 2013), each of the 28 plot locations contains a 400m^2 circular plot that has the diameter at breast height (DBH) and species of every tree (above 9cm DBH) recorded. The height of tree and height to crown was measured for every third tree in the plot. Species-specific DBH-to-height regression models were derived from the measured trees then applied to impute tree and crown heights for unmeasured trees in the plot (Mehtätalo et al., 2015). Each plot was then assigned a structural and successional stage based on visual interpretation, as outlined in the BC Government Field Manual for Describing Terrestrial Ecosystems (Province of British Columbia, 2015).

Additionally, the forest was segmented into three layers, dominant/co-dominant layer, intermediate layer and a layer for trees below 2 m. Cover (in %, rounded to the nearest multiple of ten) was also visually assessed for the three vertical layers.

Nested and centered within the circular stand inventory plots, a 10x10m square plot was used to record and map CWD information (Figure 3). This square plot was then gridded into 2m squares to aid in accurately mapping the spatial location, length and orientation of CWD pieces. All pieces of CWD over 8cm diameter, trees, shrubs and stumps were mapped within each gridded subplot. Each log was then visually assessed and given one of four bark decay and vegetation growth classes to assist in aging the CWD, similar to the aging strategy implemented by Farnell et al. (2020). Class zero represents 0-10% vegetative growth or bark present on the log, class one represents 10-50, class 2 represents 50-90% and class 3 90-100%. For each piece of CWD, height above ground was measured at each end or at the point the log exited the plot, overall length was measured between these same points. CWD pieces that were more than 50% buried were not counted in data collection.

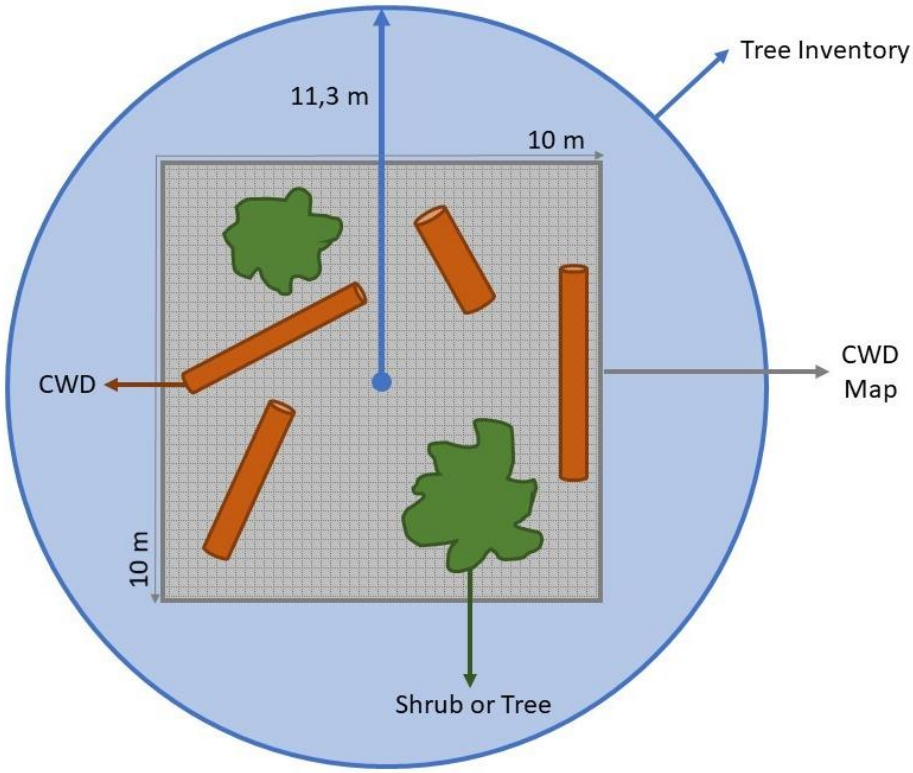

Figure 3. Example of sampling plots and CWD map. Tree inventory extent displayed in blue. The extent of the CWD map and example features are displayed within the grey square.

Chapter 3: Detection of Sub-Canopy Forest Structure Using Airborne LiDAR

3.1. Introduction

In forested systems, distinct aspects of forest structure occur at definable scales (Angelstam 1996; Bunnell 1995; Holling 1992). Resident species have adapted to persist within the structure and composition that result from natural disturbance regimes (Bunnell 1995; Holling 1992; Hunter 1999). Forest succession that is influenced by these regimes may be categorized into structural stages that describe, in part, the development of and relation between an overstorey main canopy and a developing understory sub-canopy (Province of British Columbia, 1998; Martinuzzi *et al*., 2009). While attributes and structural patterns associated with the forest canopy are well documented, less is known about the sub-canopy or understory structure (Wing *et al*., 2012). The sub-canopy consists of many structural elements such as sub-dominant trees, regenerating saplings of shade-tolerant species, shrubs, herbs, snags and coarse woody debris (Connell et al., 1997). The size, density and composition of these sub-canopy structural elements aids in the structural characterization of overall forest structure. In this chapter I primarily focus on trees that are not part of the canopy but are taller than shrubs as these trees are considered to be the sub-canopy structure of the forest.

Forest health and timber production are particularly important like British Columbia, Canada, where forestry is a major economic driver (Bourgeois 2004). A critical component of sub canopy structure are the intermediate-sized trees that exist beneath the main canopy. These sub-canopy trees represent the future forest canopy and have value for future timber supply if maintained during first-pass harvesting (Coates, 2012). Tree regeneration rate is a sub-canopy process

indicative of forest health (Rogers, 2002); another important component in forecasting possible timber supply (Korpela *et al*., 2012). More in-depth knowledge on regeneration trends will allow for more accurate assessments of harvest outlooks. Forests in British Columbia have been severely affected by the mountain pine beetle outbreak, which killed a large percentage of canopy trees (Coates, 2012). Management focus has now turned to the structure and composition of the sub-canopy to assess the remaining healthy trees and their potential contribution to future timber supply (Coates *et al*., 2006; Amoroso *et al*., 2013).

Field-based data collection provides the best description of sub-canopy attributes, however field approaches are labour and financially intensive (Hall, 2005). Alternatively, remote sensing technologies such as ALS have proven effective at measuring 3-D forest attributes across wide spatial extents (Lefsky, 2002). The major advantage of remotely sensed data is the ability to extract spatially explicit information from a broad landscape in a time-efficient and cost-effective manner (Lim, 2003). Considering the canopy intercepts a large number of LiDAR pulses, secondary-structure trees are conceptually more difficult to identify than canopy trees. However, discrete-return ALS can penetrate the canopy and accumulate up to six returns per pulse providing spatial detail on sub-canopy structures. While difficulties exist surrounding the ability to isolate where the canopy ends and the sub-canopy begins (Chasmer et al., 2006), ALS has demonstrated success when utilized to model understory characteristics including snags and shrubs (Martinuzzi *et al*., 2009; Nijland *et* al., 2014), vegetation cover (Goodwin et. al., 2007), vegetation density (Campbell et al., 2018) and forest successional stages (Falkowski *et al*., 2009). Additionally, ALS has been combined with multispectral imagery to generate understory fuel models (Jakubowksi, et al., 2013, Multu et al., 2008). These studies highlight the ability of ALS to isolate sub-canopy attributes, especially in the lowermost sections (0-4m). Furthermore,

this indicates potential of ALS based technology to assess the sub-canopy with a goal of developing a sub-canopy forest inventory.

A sub-canopy inventory in British Columbia would have a number of important management applications including forecasting forest health, timber supply, fire susceptibility, wildlife habitat quality, and carbon sequestration. Given these potential applications, coupled with advancements in availability and density of ALS data, there is an obligation to examine how well ALS can describe the structural characteristics of the sub-canopy. In this chapter I will investigate the following questions:

1. *What is the process for deriving field-based sub-canopy structure measurements from an ALS point cloud?*

Considering forests are complex ecosystems that are made up of more than just the canopy (Franklin *et al*. 2002), a successful analysis of the sub-canopy from an aerial source requires a differentiation of the attributes of the main canopy and the sub-canopy. Due to the variation of canopy height present in naturally regenerating forests (Kral *et al.*, 2010), a fixed height threshold is unlikely to be representative at a landscape scale. In order to capture this variability, there is a need for a procedure which provides a relative canopy height definition on a stand-level scale.

2. *How well can ALS metrics describe the sub-canopy characteristics of forest stands in central British Columbia?*

After isolating the sub-canopy portion of the point cloud, I will quantify volume, basal area and number of trees and will construct models to predict these sub-canopy attributes. These attributes

aim to describe the sub-canopy trees that are well-established to become a part of the canopy and play an important role in future forest succession (Pyke and Zamora, 1982). Alternatively, from a harvesting perspective, retaining sub-canopy trees will preserve the later, more commercially valuable, successional stages of forests (Leemans, 1991). Predicting information on the structural makeup of the sub-canopy using ALS could guide forest management planning and practices to focus on tree vigor to produce more valuable forest stands.

3. *How does sub-canopy structure vary across the landscape?*

Using the predictive models from research question 2, I will assess spatial distribution of sub-canopy attributes relative to climatic variants and topography. Landscape-level interpretations of sub-canopy structure are required for tactical assessments of the interaction of forest attributes with disturbance regimes, and to prudently integrate wildfire risk reduction with planning for carbon sequestration, timber supply, the establishment of climate-adapted regeneration and management of wildlife habitat. Sub-canopy trees often become ladder fuels, allowing surface fires to spread to the canopy and become full-fledged crown fires (Helms 1979; Buckley 1992). Given the recent increase and predicted future increase in the number, extent and severity of fires in western North America (Schoennagel *et al*., 2017), the ability to identify those areas with greater fuel loads and susceptibility to crown fires is needed. Mapping areas of high fuel load in the sub-canopy could pinpoint where common fire-reduction strategies such as understory thinning (Agee, 1996) should be taking place. Knowledge about where to spatially concentrate fire-reduction efforts can help protect communities and infrastructure in fire-prone regions.

In addressing these questions, I aim to assess the feasibility of using ALS to predict sub-canopy attributes and develop the predictive models capable of mapping these attributes at a landscape level to improve the allocation of resources for integrated forest management.

3.2. Materials and methods

3.2.1. Sub-canopy structural definition

In order to properly characterize the sub-canopy, I first established a consistent definition of the focal stratum. Sub-canopy structural elements of a stand were defined as trees taller than 2 m but of shorter stature than the sub-dominant component of the main canopy. These canopy layers are established in relation to each other based on the mean height of the co-dominant layer (Figure 2). Vegetation below these canopy levels and still above 2 m are considered sub-canopy structure. Main canopy height is variable due to stand age and site quality and therefore needs to be defined on an individual stand level based on relative metrics as opposed to a predetermined height. Therefore, to establish the origin of the co-dominant canopy layer, Lorey's mean height (HL) (Equation 1) was used (Table 2). This incorporates height and basal area, giving more weight to trees with a larger DBH, which are more likely to be part of the canopy (Husch et al. 1982). Several studies (Hyyppa *et al*., 2001; Naesset, 2002; Maltamo *et al*., 2006) utilize HL as it can provide a much more representative description of the canopy, regardless of unusual stand structure or outstanding maximum canopy height. Figure 4 provides an example of a stand and how trees would be classified into the canopy.

Equation 1. Lorey's Mean Height where g is basal area and h is measured tree height.

$$HL = \frac{\sum g * h}{\sum g}$$

Table 2. Canopy and sub-canopy definitions relative to HL.

Canopy Class	Definition
Dominant	>110 % of HL
Co-dominant	90-110% of HL
Sub-dominant	70-90% of HL
Sub-canopy	< 70% of HL

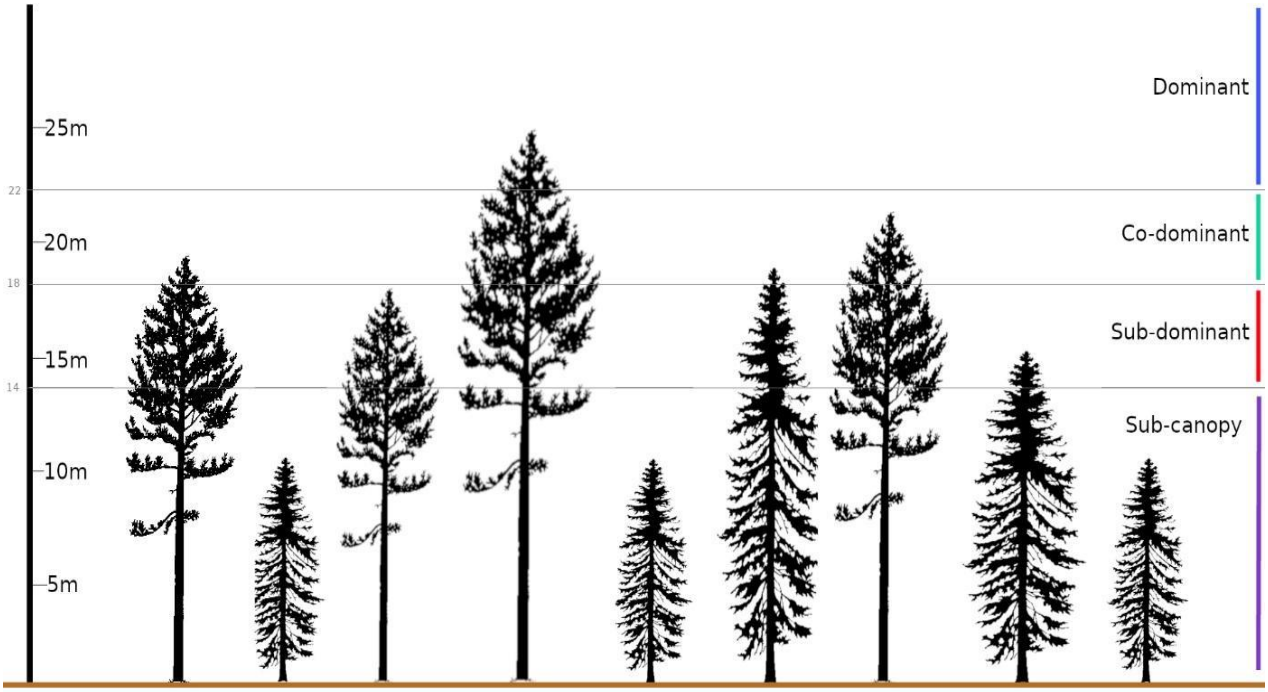

Figure 4. Canopy stratification for determining sub-canopy structure

Using our ground height and DBH measurements, HL was calculated for each plot and applied to the canopy definition as the center of the co-dominate canopy. This determined which trees in

the plots were considered sub-canopy structure for the focus of our analysis. After establishing which trees represented the sub-canopy, three variables were derived to describe sub-canopy structure. The first variable was the number of trees (N_{SC}) that were considered part of the sub-canopy (i.e. not part of the canopy and greater than 2m tall). The second variable was basal area of all sub-canopy trees in meters squared (BA_{SC}). Basal area is the cross-sectional area of a tree at 1.37 meters and was derived from our DBH measurements (Whitehead, 1979). The third variable was the volume of all sub-canopy trees in meters cubed (V_{SC}), which is calculated by multiplying basal area by measured height. These variables were then calculated for the 28 sample plots across the study region. Using these variables two sets of modelling approaches, retained canopy modelling and removed canopy modelling, were tested to compare field-based sub-canopy structure measurements to the metrics derived from the point cloud.

3.2.2. Canopy modelling

3.2.2.1. Retained-canopy modelling

To establish a baseline for quantifying sub-canopy forest inventory attributes that is consistent with current literature (Irwin, 2018; Kramer et al., 2014; Martinuzzi et al., 2009; Clark et al., 2004) the unsegmented canopy ALS point cloud was used. First, an area-based approach (ABA) was implemented for predicting the N_{SC}, BA_{SC}, and V_{SC} at a 20 x20m grid cell resolution. When using ABA, statistical models are created to relate ALS data at the cell level to the desired forest inventory attributes measured at ground plots. These models are then applied across the area of ALS coverage to obtain wall-to-wall estimates of the attributes (White et al., 2013). A suite of metrics were calculated that describe four elements of the forest stand: height, height variability, cover, and structure (Table 3). Height, and height variability metrics are commonly used for

predicting basal area and tree volume (Ferster *et al.*, 2009; Babcock *et al.*, 2012), while cover metrics can provide insight about gaps and canopy influence (Falkowski *et al.*, 2009). Lastly, structural metrics including vertical complexity index (VCI) and vertical rumple, segment the point cloud into voxels for assessment of vertical structure variance (Tompalski *et al*, 2015). All metrics were tested for multicollinearity and removed from analysis if correlation to another metric was greater than 0.8. These metrics were then used to develop predictive linear regression models for N_{SC}, BA_{SC}, and V_{SC}. Models were developed by testing all combinations of uncorrelated metrics through a forward-stepwise regression using 10-fold cross-validation while withholding 30% of plots for validation. The final models chosen for each sub-canopy variable produced the combination of lowest root-mean-square-error (RMSE) value and highest r^2 value when cross-validated.

Table 3. ALS Metrics and associated classes tested to predict sub-canopy variables

Metric	Description	Source	Category
P*n*	Height of the n^{th} percentile of returns (*n* = a single value multiple of 5, up to 95)	Roussel and Auty, 2019	Height
Max	Maximum height return	Roussel and Auty, 2019	Height
St_Dev	Standard deviation of return heights	Roussel and Auty, 2019	Height Variability
Skewness, Kurtosis	Skewness and Kurtosis of return heights	Roussel and Auty, 2019	Height Variability

Mean, Median, Mode	Mean, median and mode of return heights	Roussel and Auty, 2019	Height Variability
Above_Mean	Percentage of returns above mean	Roussel and Auty, 2019	Height Variability
Above_Median	Percentage of returns above median	Roussel and Auty, 2019	Height Variability
Cumu_%	Cumulative percentage of return heights in the lowest 10, 20, 30, 40, 50, 60, 70, 80, and 90% respectively	Roussel and Auty, 2019	Cover
P_D_2, P_D_5, P_D_10, P_D_15	% Density above 2, 5, 10 and 15m height returns respectivly	Isenburg, 2014	Cover
All_Above_ t2, All_Above_ t5, All_Above_ t10, All_Above_ t15	Total number of returns above 2, 5, 10 and 15m respectively	Isenburg, 2014	Cover
LAD_Min, LAD_Max, LAD_Mean	Minimum, maximum and mean leaf area density	Bouvier et al., 2015	Structure
VCI	Vertical Complexity Index - Distribution of abundance of returns in 1m height bins	Van Ewijk et al. 2011	Structure
Vertical_Rumple	Measure of variance of vertical structure as a function of filled voxels in point cloud	Tompalski, 2015	Structure

3.2.2.2. Removed-canopy modelling

The second modeling approach utilized a LiDAR-based approach for removal of the canopy. Since the sub-canopy definition was defined using HL, a model was generated to predict HL from the ALS point cloud. HL has been accurately predicted by ALS in previous studies (Zhang *et al*., 2017, Maltamo *et al*., 2010) and most often uses upper height metrics such as the 95^{th} percentile of height returns (P95) as a predictor variable (White *et al*., 2017). This relationship was then implemented through linear regression to develop a model for predicting HL using P95. I then applied the ABA by generating wall-to-wall metrics for P95 and apply our model to generate a raster of predicted HL across the study area at 20 x 20m grid cell resolution (White *et al*., 2013).

The resulting raster of predicted HL was then used as an input for the canopy threshold calculation and the corresponding result used as a filter that removed the canopy from the point cloud across the study region. This ensured the canopy was removed based on stand characteristics at a stand level, i.e. 20 x 20 m. The same suite of metrics (Table 3) were then generated for each plot and an ABA applied for the removed canopy using the forward-stepwise regression and 10-fold cross-validation approach to develop relationships between N_{SC}, BA_{SC}, V_{SC} and ALS derived metrics. Lastly, a test for significance between modeling procedures was conducted by using a two-sample t-test on the residuals of predicted values produced from both modelling methods for each NSC, BASC and VSC.

3.2.3. Spatial distribution

Results of both modelling approaches were compared to determine if retaining or removing the canopy produced more accurate models for each sub-canopy variable. The ABA was then applied using the strongest models and a predictive map was then produced for each variable across the entire study region. Lastly, these maps were overlain with BGC variant mapping to visualize how sub-canopy variables vary in relation to known forest attributes and topographical variation at the landscape scale.

3.3. Results

3.3.1. Sub-canopy composition

The field-based definition of the sub-canopy using HL coupled with the structurally guided sampling approach successfully produced plots with a variation of sub-canopy composition (Figure 5). The canopy -- sub-canopy threshold for the plots ranged from 6.7m to 14.3m. The number of trees considered part of the sub-canopy range from 0 to 30, while the percentage of trees in the plot that were considered sub-canopy trees varied between 0 and 55%. Notably, plot 25 which was composed of the highest P95, average height and low CoV, had considerably higher sub-canopy volume compared to other plots.

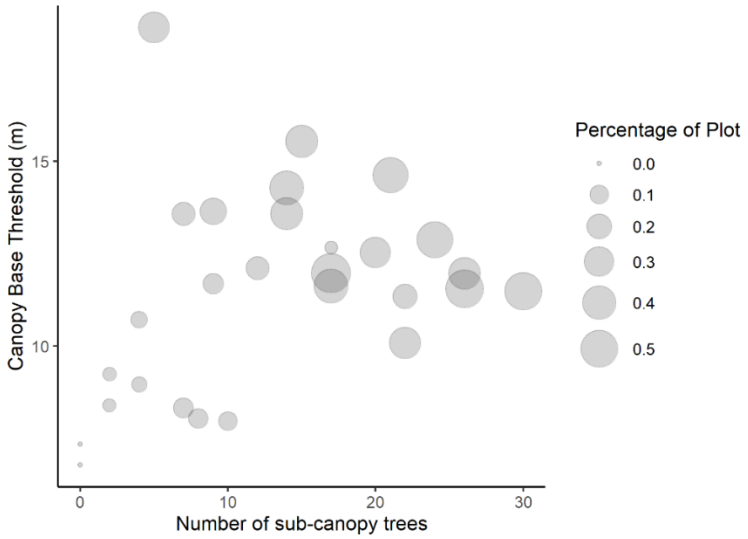

Figure 5. Summary of sub-canopy structure within the 28 ground plots using canopy case height, number of sub-canopy trees and percentage of trees classified as sub-canopy.

Figure 6 displays the linear regression model using P95 to predict HL (r^2 = 0.96, RMSE = 0.73m) for the 28 ground truth sites. The strong performance of the model indicated HL could be confidently estimated from an ALS point cloud.

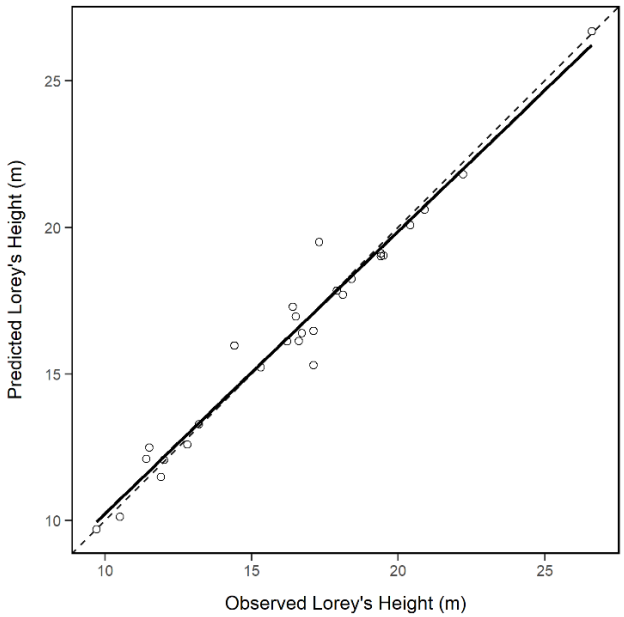

Figure 6. Predicted vs. observed HL using a linear regression model. Regression line displayed in black and 1:1 line displayed as dashed line.

3.3.2. Sub-canopy models

Table 4 describes the metrics used in the strongest performing models for each sub-canopy variable for both modelling approaches. When the canopy was removed, only metrics from the height and structure classes were selected. When the canopy was retained, there was a more diverse selection across metric classes including height variability and cover.

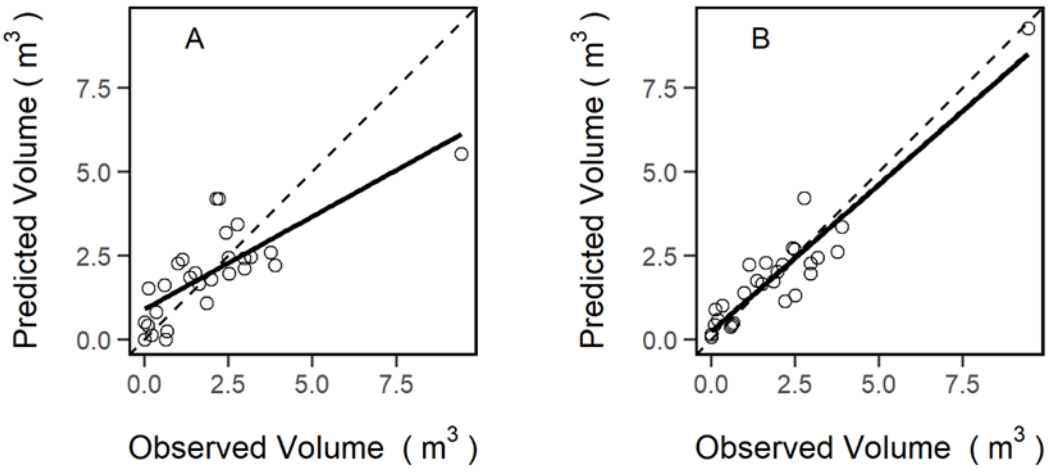

Figure 7 Linear regression results for predicting sub-canopy volume using A) Canopy retention B) Canopy removal. Regression line displayed in black and 1:1 line displayed as dashed line.

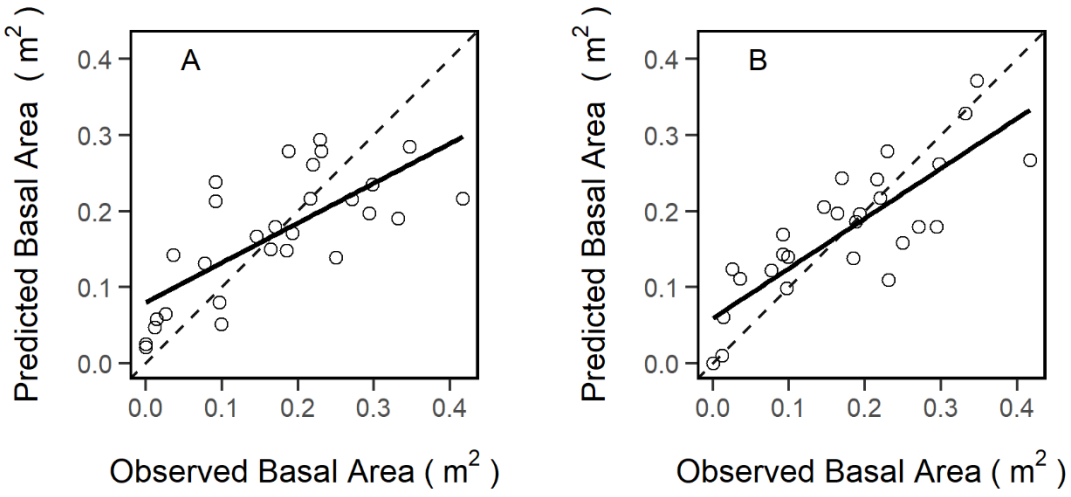

Figure 8. Linear regression results for predicting sub-canopy basal area using A) Canopy retention B) Canopy removal. Regression line displayed in black and 1:1 line displayed as dashed line.

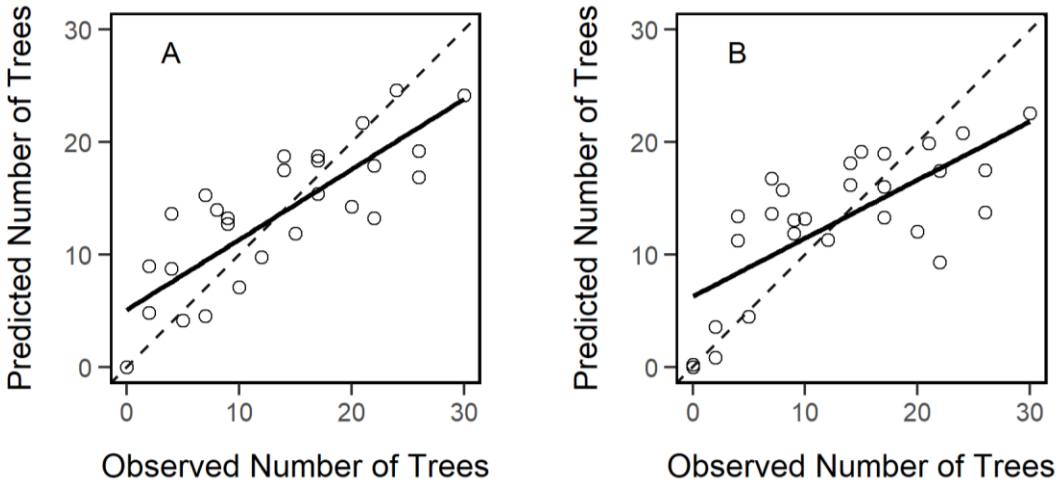

Figure 9: Linear regression results for predicting number of sub-canopy trees using A) Canopy retention B) Canopy removal. Regression line displayed in black and 1:1 line displayed as dashed line.

Removing the canopy resulted in stronger predictive models for two-thirds of the variables when compared to using the retained canopy approach (Table 4). Sub-canopy tree volume (Figure 7) using the canopy removal approach was the most accurately predicted (r^2 = 0.88, RMSE = 0.654 m^3, Bias% = 0). When the canopy was not removed the predictive capability dropped considerably, RMSE nearly doubled and small overestimation was present (r^2 = 0.57, RMSE = 1.21 m^3, Bias% = 2.42). Sub-canopy basal area (Figure 8) was predicted moderately well when the canopy was removed (r^2 = 0.68, RMSE = 0.064 m^2) and not as strongly when the canopy was retained (r^2 = 0.52, RMSE = 0.078 m^2). Bias percentage for both basal area models was less than 1%. Prediction trends when removing the canopy indicated an overestimation of stands with

lower basal area and an underestimation with stands with greater basal area. This trend also occurred in the number of trees and basal area canopy removal models (Figure 9). Additionally, Figure 7 indicates that as opposed to volume and basal-area, predictive strength for number of sub-canopy trees was stronger when the canopy was retained (r2 = 0.59, RMSE = 5.436 trees) compared to when it was removed (r2 = 0.55, RMSE = 5.892 trees).The retained model had a small bias percentage of 1.45% while the removed canopy model had almost none (Bias% = 0.05). All predictor variables for each model were significant (95% CI). Significance testing between the residuals of the retained and removed canopy models found the removed canopy model for volume to be significantly different (p = 0.049), while basal area and number of trees not significantly different (p = 0.621 and p = 0.915). Statistics were completed using R 3.5.0 (R Core Team, 2018), and the *caret* (v6.0-84; Kuhn, 2008) package.

Table 4. Summary of regression model statistics.

Model	Predictor Variables	R^2	RMSE	RMSE%	Bias%
V_{SC}- Removed	Max LAD_max P_D_15	0.88	0.654	34.04%	0.00%
V_{SC}-Retained	P95 Above_median	0.57	1.21	63.02%	2.42%
BA_{SC}- Removed	Vertical_rumple LAD_Max Mean	0.68	0.064	38.29%	0.91%
BA_{SC}- Retained	St_Dev	0.52	0.078	46.57%	0.00%

N_{SC} - Removed	Vertical_Rumple LAD_Max P_D_15	0.55	5.892	45.32%	0.05%
N_{SC}- Retained	P15 All_Above_Mean All_Above_t5	0.59	5.436	41.82%	1.45%

3.3.3. Landscape distribution

Figure 10 displays the use of the strongest performing model, to generate a predictive map of sub-canopy tree volume for the study area at a 20m grid resolution. The central region of the study area contains the most sub-canopy volume. High levels of sub-canopy volume also appear at the lower elevations, specifically in valleys. Figure 8 also contains the two climatic zones present in the study site. The Sub-boreal spruce variant indicates considerably more sub-canopy volume compared to the Engelmann spruce-subalpine fir variant.

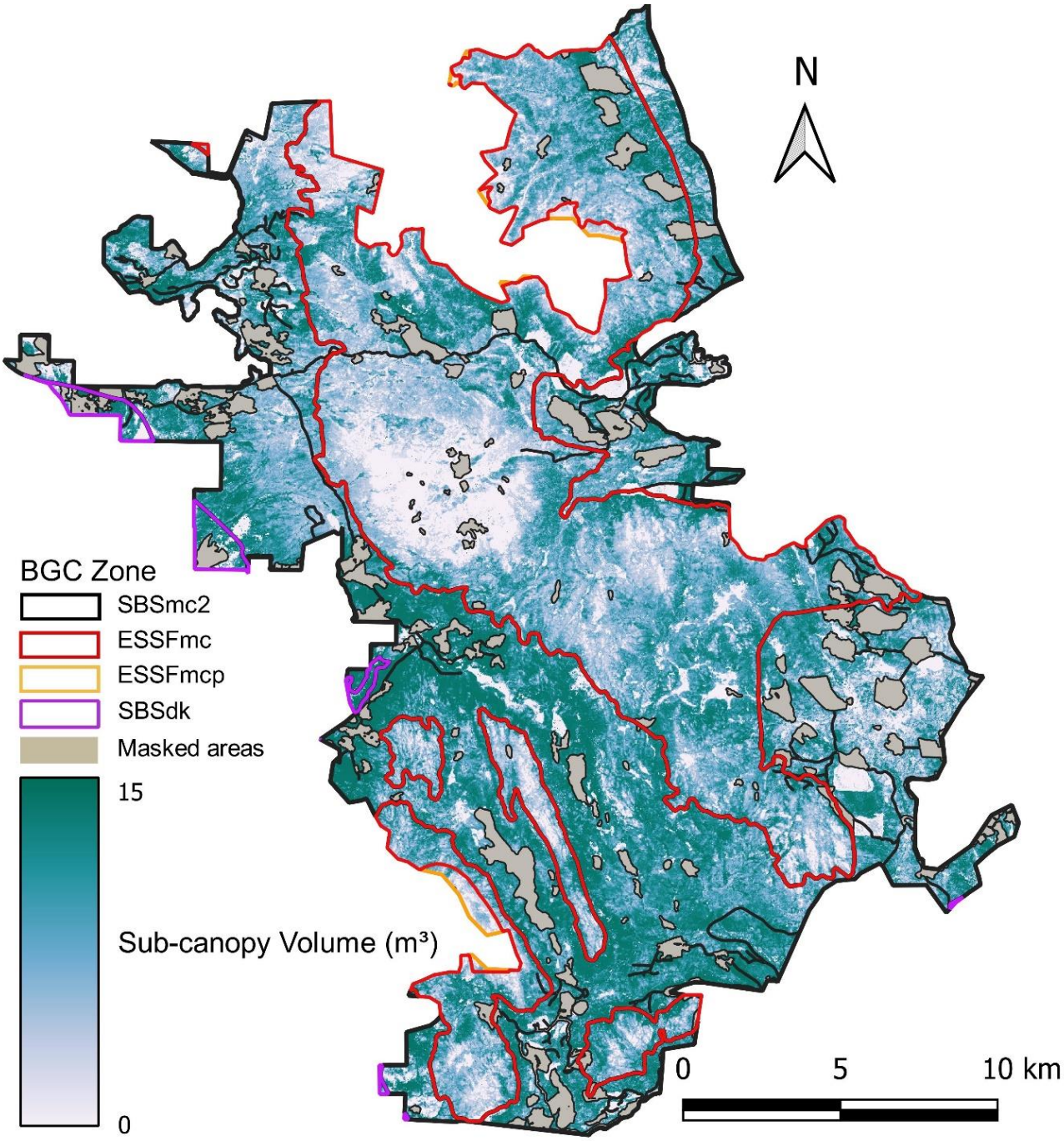

Figure 10. Predicted sub-canopy volume of Deception Lake overlain with local BGC variants. ESSF variants represent higher elevations while SBS variants represent lower elevations. Areas in white are either recently harvested, roads or water and are masked for evaluation.

3.4. Discussion

3.4.1. Sub-canopy description

To address research question one, I created and assessed a methodology for removing forest canopy from an ALS point cloud to examine sub-canopy structural characteristics. I exhibit that by using the 95th percentile of a point cloud HL can be accurately predicted. This is consistent with others who have been able to predict HL from ALS metrics with similar accuracy (e.g., Holmgren, 2004). Using predicted Lorey's mean height as a baseline for a percentile-based canopy threshold enabled us to differentiate the sub-canopy at the stand level, and address the natural variability in canopy structure between stands. Agca *et al.* (2011) also used HL to calculate canopy base height at the stand level and found it to be an effective method. Within my study, removing the canopy using this method increased the accuracy of the two best predicted sub-canopy variables, volume and basal area. While a single canopy height cannot be uniformly representative of a 400-m^2 stand, these results indicate that our canopy separation procedure removes a substantial portion of the main canopy and allows an improved assessment of sub-canopy basal area and a significantly better assessment of tree volume.

3.4.2. ALS characterization

The sub-canopy models indicate the capability to predict sub-canopy structural variables with reasonable accuracy using ALS-derived metrics. Our second research question is addressed in particular by the strong prediction of key forest inventory metric, sub-canopy volume. Prediction accuracy ranged depending on the variable and maintenance of the canopy structure. Two models, sub-canopy volume and basal area, performed better with the canopy removed and explained 88% and 68% of the variation in the data respectively. Total stand volume and basal

area are highly correlated (Naesset, 1999) and our results imply sub-canopy volume and basal area are likewise correlated. These models share a predictor metric (LAD_Max) highlighting its importance in describing the sub-canopy. Height metrics in both models establish the upper threshold of the sub-canopy, while LAD_Max represents the variation and density of structure within. This coincides with previous studies where LAD metrics proved to inform on the vertical heterogeneity of sub-canopy vegetation (Bouvier *et al*., 2015) while upper percentile height metrics excel at predicting volume and basal area (White *et al*., 2017). Sub-canopy volume was likely predicted better compared to basal area due to tree volume being a direct function of height. This is reiterated by the significance testing between models where the removed canopy volume model is significantly stronger than the retained canopy model. Alternatively, the removed canopy basal area model has a better fit (r^2 and RMSE) than the retained canopy model, but is not significantly different in predictive accuracy. Overall, these findings exhibit requirement for both height and structure-based metrics for accurate representation of the sub-canopy.

Number of trees present in the sub-canopy was the weakest performing model with the canopy removed ($r^2 = 0.55$). This was expected given previous difficulties in counting and segmenting understory trees with a point cloud density of less than 170 points per square meter (Hamraz *et al*., 2017). However, this model performed marginally better when the canopy was retained ($r^2 = 0.59$) which was unexpected given the improved performance of the volume and basal area models without the canopy. This may be due to the spruce and subalpine fir trees growing in clumps which affects habitat and potential growth value (B.C. Ministry of Forests, 1998). Our models are able to predict volume and basal area of these clumps but lack the density to identify individual trees. Removing the canopy in this situation would further lower the density and

possibly explain the poorer performance of the removed canopy model. Alternatively, the retained canopy model which maintains a comparatively higher agreement exhibits a noticeably different composition of metrics (All_Above_t5, P15 and Above_Mean). By utilizing two cover-based metrics and a lower percentile height metric, the model is able to form a relationship between canopy cover and quantity of sub-canopy trees. This is similar to Latifi *et al*. (2016) who indicated that prediction of intermediate forest layers are correlated to canopy cover metrics. While our model appears to estimate the general proportion of sub-canopy trees correctly, the remaining uncertainty surronding the number of trees is likely due to the inability of ALS metrics to perform segmentation of these tree clumps at a 20 m scale. This is agreeable with Yin et al. (2019) who suggest that for individual tree segmentation, pixel size must be at least one quarter of the crown diameter.

3.4.3. Distribution

Our final research question was addressed by Figure 8, where patterns of sub-canopy volume become evident at the landscape scale. Areas with high levels of sub-canopy volume stand out in the valleys and flatter terrain. This relationship is especially visible by the lower volume found in the higher elevation and more rugged ESSF variant compared to the SBS variant (Meidinger and Pojar, 1990). The comparatively shorter and cooler growing seasons of the higher sections of the ESSF (Meidinger and Pojar, 1990) do not appear to develop sub-canopy structure well. In contrast, sub-canopy volume within the SBS variant is shown to be highly variable but appears in clusters or elongated shapes of high volume corresponding with the woodland subzone. This is suggestive of a relationship with one or more topographic variables, which may be partially

related to the stand level classes in the BGC classification hierarchy (i.e., site series, Meidinger and Pojar 1990) and could be the focus of future research.

3.4.4. Applications

Improved understanding of sub-canopy structure patterns can be useful for a range of tasks from harvest management planning to fire-risk assessments to planning for climate adapted regeneration and carbon sequestration. While this chapter focused on using an ABA, there is potential to apply individual tree segmentation approaches after implementing the canopy removal strategy. From a timber supply perspective, sub-canopy volume in the understory have shown positive growth responses when sections of the canopy have been removed (Hawkins *et al.*, 2013). By retaining sub-canopy structure, the subsequent successional stages are preserved, capturing additional commercial, carbon or microclimate value (e.g., Leemans, 1991). Understory retention is also a harvesting strategy currently being implemented in boreal forests in Alberta, Canada (Charchuk, 2018).

Expanding beyond stand attributes with a timber focus, sub-canopy structure can substantially influence forest fires. As fire severity and frequency continue to increase in Western North America, sub-canopy volume can be used as an input for models predicting fire susceptibility and severity. These models often contain fuel classification layers or presence of intermediate canopy ladders fuels (Whitman *et al*., 2013; Scott and Reinhardt, 2001; Rothermel 1991). The sub-canopy attributes predicted in this chapter show potential to improve model reliability by replacing or augmenting traditional input layers, which can currently be based off of as little as normalized difference vegetation index (NDVI) values (Whitman *et al.*, 2013). Combined with other ALS fuel predictive layers (Kramer *et al.*, 2016), our predicted sub-canopy attributes

present opportunities to create more robust fire management models. These attributes can also be used as inputs into predictive ecological modeling efforts to determine stand successional stage. Other applications exist including quantification and location of sub-canopy structure for identifying habitat potential for wildlife and carbon stock modelling procedures (Hill and Broughton, 2009).

Chapter 4 – Spatial Detection and Volumetric Quantification of Coarse Woody Debris in Natural Forest Stands Using Airborne LiDAR.

4.1. Introduction

As management of the sources and sinks of carbon is increasingly recognized as a tool to mitigate climate change, efforts to quantify and predict carbon sources and sinks are increasing (Grote et al., 2011; Merganičová 2019). Forests are important carbon sinks which absorb around 30% of anthropogenic carbon emissions (Schulze et al, 2000). Coarse woody debris (CWD), defined as dead woody biomass on the forest floor with a diameter greater than a given threshold, is an important component of the terrestrial carbon cycle within forest stands (Smallman et al., 2017), with over a quarter of forest carbon stored as CWD (Pan et al. 2011). CWD, defined as residual dead woody biomass in close proximity to the forest floor with a diameter greater than a given threshold, is an influential functional and structural element of forest ecosystems (Harmon et al., 1986). Dependent on time since mortality and environmental conditions, CWD is present in a range of sizes and decompositional stages. As a single element of the overall forest structure, the amount and type of CWD is a function of the other structural elements in a stand including species composition, canopy height, sub-canopy tree density and stand age (Sturtevant et al., 1997). In natural forest stands, large volumes of CWD are generally associated with later forest successional stages (Harmon and Hua, 1991), as they are representative of trees that are no longer part of the canopy. This opens up gaps in the canopy leading to understory regeneration and increased vertical heterogeneity of forest structure (Feldmann et al., 2018). Information involving the size and volume of CWD in a stand could

provide insight into both successional and structural forest stages, as well as site-level classifications for ecosystem mapping.

CWD is often referenced as an indicator of diverse and productive old-growth stands as it represents multiple age cohorts and vertical heterogeneity (Feller, 2003; Keren and Diaci, 2018), plays an important role in carbon storage (Gough et al., 2007), providing habitat for a range of wildlife (McComb, 2003; Ucitel et al., 2003) and wildfire fuel load (Cansler et al., 2019; Choi et al., 2015; Aponte et al., 2014). Considering these relations, the presence of CWD contributes to the maintenance of heterogeneous structural and biological diversity.

Developing reliable CWD estimates and inventories has multiple challenges (Woodall et al. 2008, Campbell et al. 2019). The volume and mass of CWD in forests is highly variable across stand types, successional stage, climate, disturbance history and forest management regimes (Harmon et al. 1986). Conventional efforts to detect CWD often rely on site-specific and intensive field-based measurements which can be time-consuming. Jordan et al. (2004) for example, reports an average time of 90 seconds to measure end diameters, length, species and decay class for a single piece of CWD. Old and decomposed logs can prove difficult to measure as the majority of the log may be buried in the forest floor, complicating diameter measurements. Additionally, smaller CWD pieces are often tapered and only partially meet the requirements to be recorded as CWD. Accessibility can also prove to be an obstacle for CWD field-measurements as large CWD may extend over multiple shrubs and ground depressions, further adding to the difficulty of hand measurements. Given the increasing importance of reliable estimates of CWD; novel, accurate and cost-effective inventory methods are needed. Remote sensing methods have to potential to improve CWD inventories (Pan et al. 2011).

Airborne laser scanning (ALS) presents an opportunity to obtain spatially explicit information over broad landscapes in a manner considerably more time-efficient and cost-effective when compared to field-based CWD measurements. The number of ALS pulses to reach the forest floor is influenced by overstory canopy cover, height, density and shrub presence (Venier et al., 2012). Despite this, detection of understory vegetation, CWD, as well as attributes of the forest floor are able to be consistently detected and as a result ALS has been shown to provide detailed three-dimensional representations of the canopy (White et al., 2018), sub-canopy (Jarron et al., 2020), and understory attributes (Campbell et al., 2018). This characterization of both vertical and horizontal structure provides ALS with a substantial advantage over other remotely sensed data such as aerial photography and satellite imagery, which are restricted to assessing forest structure based on upper canopy attributes.

The three-dimensional capability of ALS have resulted in widespread use of the technology worldwide to map forest attributes including habitat structure (Coops et al., 2016), tree health (Shendryk et al., 2016) and standing dead snags (Wing et al., 2015). However, comparatively less research has focused on detection of ground-level woody biomass using ALS. The ability to identify and characterize more detailed ground-level forest attributes will improve as the average ALS point return density continues to increase. Table 5 summarizes recent studies that focus on using ALS to delineate or quantify CWD.

Table 5. Summary table of recent studies focusing on CWD detection and quantification.

Author	Location	Forest type and condition	Point Density	Method	Height Thresholds	Findings
Pesonen et al. (2008)	Finland	Mixed-wood; Natural stands. Leaf-off conditions	4 points/m^2	Generated ALS-derived metrics to establish a relationship between metrics and plot level CWD volume.	Lower: 10cm Upper: Canopy	Applied a mixture of height and intensity metrics to establish predictive model (R^2 = 0.61, RMSE% = 51.6%)

Queiroz et al. (2020)	Alberta, Canada	Mixed-wood Boreal; disturbed. Leaf-on conditions.	11 points/m^2	Used optical imagery derived form multispectral ALS to generate predictive models for CWD volume.	Lower: 0cm Upper: 100cm	Successful models were developed (R^2 = 0.62) and use to generate predictive maps for the study area.
Blanchard et al. (2011)	California, USA	Open site with recent fire site; minimal canopy cover. Low density vegetation conditions	10.5 points/m^2	Created fine-scale raster layers derived from ALS data and employed an object based image analysis to detect CWD.	None	73% of measured logs were detected. Over classification was present in areas with vegetation and tree canopy.
Lindberg et al. (2013)	Sweden	Managed hemi-boreal; site recently hit by storm. Leaf-on conditions	69 points/m^2	Used a line template matching algorithm to vectorize and directly match the point cloud to 651 field-measured CWD and produced a raster displaying support levels for each line as a detected log.	Lower: 20cm Upper: 100cm	48% of the field-measured CWD could be directly linked to detected lines. Issues with complex overlap of CWD and false positives with other linear ground features and dense vegetation cover.
Joyce et al. (2019)	Minnesota, USA	Managed, Mixed forest; leaf-off conditions	25 points/m^2	Used height thresholds to isolate CWD and manually inspected the point cloud for logs.	Lower: 0cm Upper: 130cm	Manually detected 23% of known CWD. Developed logistic regression models describing how log and site attributes influenced detection rates. Detection rates surpassed 50% when logs were > 30cm diameter and pulse density > 7 pls/m^2
Nystrom et al. (2014)	Sweden	Managed Boreal forest; wind throw site. Leaf-on conditions	65 points/m^2	Established the height difference between two elevation models and combines that layer with a line matching template to detect individual logs.	None	38% of wind thrown trees were detected, larger trees detect at higher percentages. Large commission errors related to linear ground elements such as shrubs and ditches.

For ALS data collected during leaf-off conditions, studies have found that shrub cover and density do not have a significant impact on CWD detection (Seielstad and Queen, 2003; Pesonen et al., 2008; Joyce et al., 2019); principally because studied shrubs are deciduous in nature. The ALS data that were acquired during leaf-on conditions, indicate that leafy shrubs can complicate CWD detection (Nystrom et al., 2014; Lindberg et al., 2013). As such, a method is required to filter out shrub returns from CWD returns that likely occur within the same vertical stratum (Wing et al., 2012).

As shown in Table 1, the majority of studies of CWD detection using ALS have occurred in open canopy conditions or leaf-off canopy conditions which are ideal for increased density of returns

lower in the canopy and from the forest floor. While useful for assessing CWD after disturbances, most natural forests contain much denser canopies. Canopy occlusion can severely reduce the number of ALS returns that reach the lower levels of a forest stand, and has been highlighted as a significant limiting factor when characterizing understory structural elements (Hill and Broughton 2009; Morsdorf et al., 2010). As a result, CWD under dense canopies is more commonly estimated using indirect volume modelling such as the ABA applied in Chapter 3 (Pesonen et al 2008.; Van Aardt et al., 2011) were statistical models relate point cloud distributions within a given area to plot level volume estimates of CWD. Interpretations based on manual identification of CWD within a height-filtered point cloud have also been implemented to quantify CWD (Joyce et al., 2019). Quantification of this sensitivity to point density is presented in relation to CWD by Joyce et al. (2019) who demonstrate that CWD detection rates surpassed 50% when understory pulse density reached 7 pulses per m^2.

Given the important role of CWD in the terrestrial carbon cycle, and its important role in providing a range of ecological goods and services, coupled with advancements in availability and density of ALS data, there is an opportunity to develop new approaches to automatically detect and assess the dimension abundance of CWD across a range of forest stand types. The overall goal of this chapter therefore is to develop an automated process to detect, quantify and map CWD directly from ALS data.

4.2. Methods

To begin, I develop a methodology that identifies ALS returns likely to be associated with CWD over a range of forest structural classes during leaf-on conditions. Once detected, individual pieces of CWD were identified and vectorized and their dimensional and positional accuracy

assessed using digitized field maps at known CWD locations. CWD estimates were then compared to field-based measurements to assess the ability of the methodology to predict plot level CWD volume from individually mapped pieces. In addition, I assessed the influence of CWD and plot-level forest structural metrics on CWD detection rates such as canopy cover, stand density and decay state of the CWD. Utilizing the detected CWD logs, plot-level CWD volume were used to estimate ALS derived height and length measurements directly from the detected logs. Lastly, I implement the method over a forest management area covering a range of different structural attributes to generate maps of estimated CWD volume, allowing the examination of CWD variation patterns within and between forest stands.

4.2.1. Plot refinement

Given the reliance on pulse density to accurately characterize understory attributes, I required plots to have a minimum average of 7 pulses/m^2 below 1 m elevation based on the recommendations of Joyce et al. (2019), resulting in 16 of the original 28 plots being suitable for analysis. Additionally, large-diameter CWD considered as greater than 30 cm in diameter (Jönsson and Jonsson 2007; Bunnell and Dunsworth, 2014), have been identified as more ecologically valuable (Arsenault, 2002) as increasing diameter is positively correlated with biodiversity (Johnson and Joshnson, 2007) with vertebrates being observed to select CWD greater than 25 cm in diameter for habitat (Bunnell and Houde, 2010) and the slower decay rates associated with large CWD having positive impacts on forest carbon stocks (Nunery and Keeton, 2010). Considering the ecological and management importance of large-diameter CWD, combined with previous CWD studies having observed successful segmentation of CWD having a minimum of 30 cm diameter (Mücke, 2013; Inoue et al., 2014; Joyce et al., 2019) we

established 30cm as the minimum diameter for detection of CWD logs in our study. Additionally, an analysis of our data showed CWD with a minimum diameter of 30cm to account for 79% of total volume across all 16 plots.

With my plots set and my targeted CWD pieces defined, a set of linked processing steps were developed to locate, map and measure CWD across the study area. These steps included: a refined ground point classification approach that minimizes the points assigned to the ground surface, implementation of point cloud height thresholds, short stature vegetation removal and lastly linear feature extraction. Each step required a small set of parameters to allow the CWD to be extracted from the full normalized point cloud.

4.2.2. Delineating CWD with ALS

4.2.2.1. Ground point classification

Given the low elevation of CWD and the tendency of near-ground returns to be misclassified as ground returns (Kim et al., 2003; Brubaker et al., 2013), it was imperative to differentiate CWD returns from ground returns to reduce the number of CWD returns lost through normalization. To achieve this, I implemented the cloth simulation filter (CSF) normalization algorithm (Zhang et al., 2016). The CSF method inverts the point cloud and simulates covering the inverted surface with a ridged cloth. Nodes in the simulated cloth are related to the ALS returns to establish the surface. If a node deviates too much from the cloth, as a CWD return may, they are excluded from the cloth and considered non-ground returns. The CSF contains a minimum threshold parameter, where returns below are revalued to 0m, allowing returns above the threshold to stand out more from the surface. Given that the minimum diameter of logs I aimed to detect was 30cm, the CSF threshold was also set at 30cm.

4.2.2.2. Point cloud thresholds

Once normalized, the point cloud was vertically segmented using a combination of lower and upper height thresholds. Previous studies have demonstrated that successful detection of CWD relies on a height-filtered point cloud (Abalharth et al., 2013; Lindberg et al., 2013; Pesonen et al., 2008). The lower threshold was set at 30cm, analogous with the CSF minimum threshold, which excluded all points classified as ground by the CSF. Next, an upper threshold needed to be established to vertically isolate potential CWD returns from other, relatively taller, understory structures. Given the majority of CWD is oriented relatively horizontal to the ground, as elevation increases the likelihood of CWD being present decreases. A visual analysis of our field measured CWD displayed 98% of logs occurring below 1m and was therefore set as the upper height threshold.

4.2.2.3. Vegetation removal

With upper and lower CWD height thresholds set, returns required separation from short-stature vegetation such as shrubs that are present in the same stratum as CWD (Wing, 2012). ALS pulses may pass through these short stature vegetative leaves by providing partial hits on small branches and twigs, creating multiple returns from a single pulse (Raber et al., 2002). These are unlikely to be CWD as Béland et al. (2014) found 81% of multi-return pulses to be associated with small branches and twigs from trees and shrubs. Alternatively, larger and denser objects such as CWD logs usually allow for only single returns from a pulse. Removing these multi-return pulses would eliminate some of the returns associated with these unwanted vegetative structures. However, some multi-return pulses may interact with the canopy and within the established height thresholds, which could still feasibly represent CWD returns. Considering this,

removing multi-return pulses must be limited to those that have multiple returns within the isolated height stratum. Therefore, to filter out potential shrub returns from our plots, pulses with multiple returns under 1m were removed.

4.2.2.4. Linear feature extraction

In the final step, linear feature extraction was undertaken to segment the isolated ALS returns into discernible linear objects. Due to the extremely high point density required for the raster-based line matching template undertaken by Lindeberg et al. (2013) and Nystrom et al., (2014) instead I utilized the approach of Olivier and Lindbergh (2015) that classifies each return as linear or non-linear relative to the neighbouring returns. Once returns classified as linear were identified, our approach transitioned to vectorization of the linear points.

To vectorize the linear returns from the filtered ALS point cloud, returns were run through a series of spatial transformations. First, the points were buffered with a distance of 60cm, twice the estimated horizontal accuracy for our ALS data (Table 2), and dissolved to create continuous elongated polygons that likely represented CWD. A centerline was then established within each polygon by constructing a skeleton polyline feature to represent the CWD. The line features were then simplified to form more ridged lines that emulate the shape of a log. In order to connect line features that are likely separated sections of the same CWD log, line features were extended two meters in both directions. If these extended lines intersected another linear segment, they were merged into a single line and simplified once again to represent a straight log. If the extension line did not intersect any other features, it was deleted and the original length of the segment was maintained. A 60 cm buffer was then created around each line segment and the resulting polygon dissolved to connect spatially close linear features that are oriented in such a way that line

extensions failed to connect them. The centerline and ridged simplification procedure were then repeated to produce the final line segments representing detected CWD. A 30 cm buffer was then generated around the final line segments and spatially overlain with the ALS point cloud to extract the mean height of returns within the buffer zone which was then divided by two to represent a constant radius of the CWD. For all plots, the volume from each detected line segment was (i.e., CWD log) summed to generate plot-level CWD volume estimates.

Lastly, this entire procedure was applied to a forest management area which has been segregated into four VRI units with different structural attributes. Each unit is of a different average age, height and species composition. Applying the methodology to these four different VRI stands provided a comparison between the known forest structures of these units and predicted volume of CWD. Given that taller and older forest stands are generally known to contain greater volume of CWD then younger smaller stands, the ALS predicted CWD volumes were assessed against this assumption.

4.2.3. Accuracy assessments

Accuracy of CWD detection was assessed at three scales; the individual CWD log level, the plot level and the stand level. First, accuracy of individual CWD log detection was evaluated by comparing known log locations and dimensions with detected line segments. Findings were then summarized in histograms displaying individual log detection relative to average diameter, maximum diameter, length, average height above ground, bark class and growth class. Second, the volume for each detected piece of CWD was summed to create a plot level estimate of total CWD volume. Estimates for each plot were then compared to the measured volume for each plot and a regression model was developed to calculate how correlated the predicted plot volumes

were with the measured volumes. To summarize the structure at each plot and its influence over detections rates, a group of ALS metrics including percent of returns classified as ground, number of multi-return pulses under 1m, canopy cover percentage and Lorey's mean height were generated to assess CWD detection rates. An unpaired t-test between detected and undetected CWD was conducted for each metric to assess for significant influence on successful detection. Lastly, when the linear object detection was expanded over the VRI polygons, the volume within each identified log was summed into a 5m raster to present a volume map across the four VRI stands. These stands vary by height, age and canopy composition. The volumes associated with the raster layer were then compared to the recorded forest structural attributes associated with each VRI stand.

4.2.4. Software and routines

Segmentation and normalization of the ALS point cloud to isolate CWD returns were completed within R 3.5.0 (R Core Team, 2018) using the "lidR" package (Roussel and Auty, 2019). The linear detection feature used within "lidR" was a boolean linear detection function called "shp_line", based on the linear detection algorithm presented by Olivier and Lindbergh (2015). The algorithm has two parameter settings that can be adjusted depending on the density of the point cloud. For consistency, the parameters for this study were set as th1= 7 and k = 8. The CWD object detection was completed within ArcMap (ESRI, 2019) and developed into an automated, single-input model.

4.3. Results

4.3.1. Individual log detection

Of the 16 plots, 12 contained CWD meeting our minimum diameter requirement while four plots did not. Across the 16 plots a total of 28 CWD logs with an average diameter 35.2 cm, average height above the ground of 39.2 cm and an average length of 4.64 m were measured in the field. Analysis of ALS-detected logs indicated that of the 28, 18 were successfully detected while 10 were not. Figure 11 provides a breakdown of how detection varied based on individual log attributes. Diameter of the log, average or maximum, did not appear to have any influence over detection rate. However, detection rate appears to increase for longer logs and logs that were more elevated from the ground. This suggests that length and height above ground are more influential in detection than is average or maximum log diameter. Level of CWD decay, measured by growth and bark classes, suggests that older, more decayed logs were detected less often. Bark Class 0 and 1 represent logs with zero and minimal bark on them. This loss of bark is a result of decomposition and CWD in these two classes are detected notably less compared to bark classes 2 and 3 which contain most and all of the bark and represent more recently fallen CWD.

The other measure of decay, increased vegetation growth on CWD, also resulted in lower rates of detection with growth classes 0 and 1, which contain no and minimal vegetative growth respectively, being detected considerably more often than those in growth classes 2 and 3 for which the majority is covered and fully covered by vegetation growth. Using an unpaired t-test the log diameter, average ($p = 0.618$) or maximum ($p = 0.964$), did not significantly influence detection rate. Increasing CWD length had a strong influence but not a statistically significant one ($p = 0.166$) while average height above ground proved to be the only continuous attribute that was significant ($p = 0.038$), with 11 of 12 logs greater than 50 cm off the ground being

detected. The strongest trends were seen across bark classes as CWD in classes 2 and 3 were detected 85% of the time compared to only 47% for classes 0 and 1. A similar trend was found for vegetation growth classes which saw CWD classified into class 0 and 1 detected 74% of the time in contrast to only 44% for classes 2 and 3.

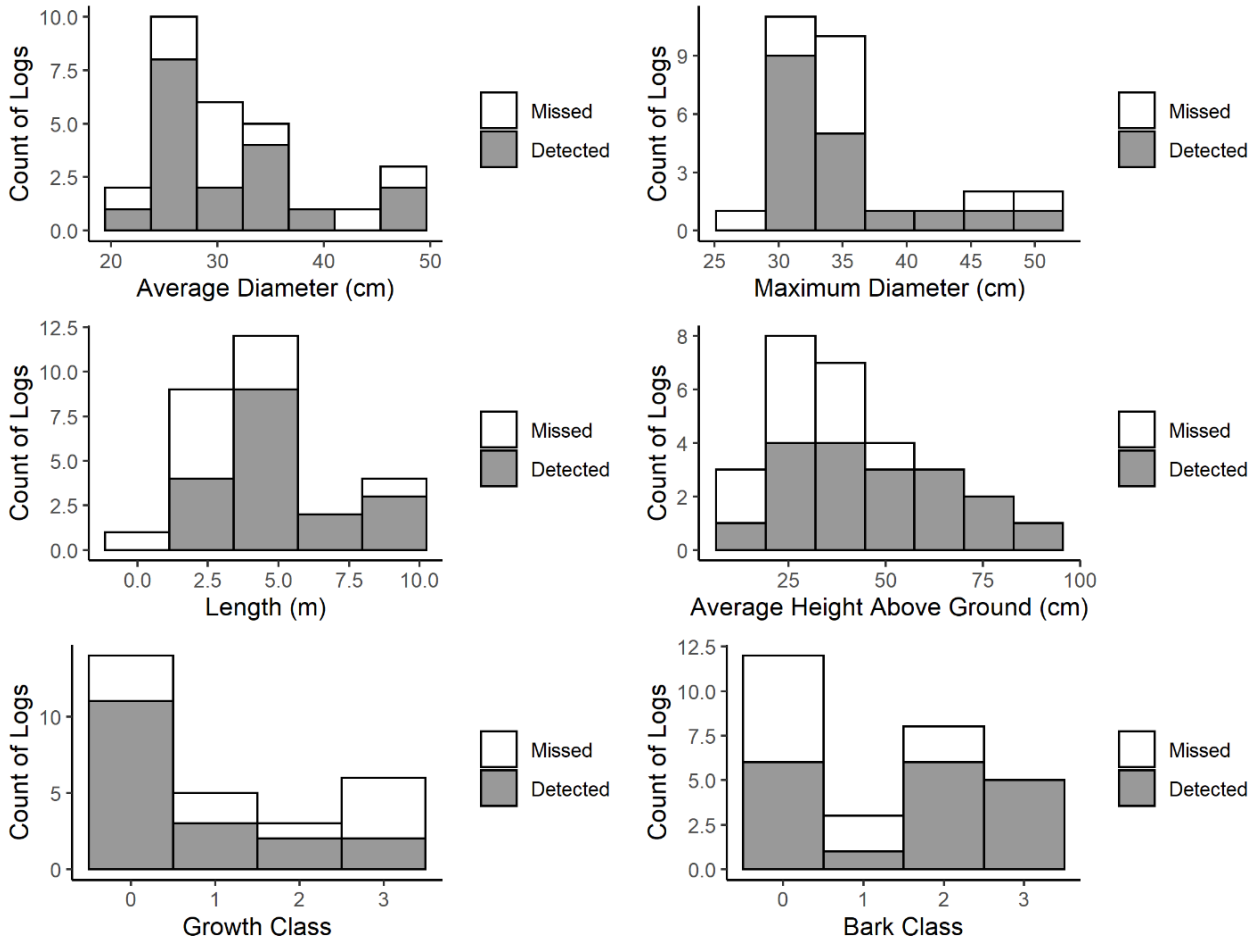

Figure 11. Distribution of measured individual CWD log attributes and associated ALS detection rates (n=28).

Figure 12 displays an example of two ecologically different plots, 16 and 35, that both presented successful detection of CWD. Plot 16 was a relatively wet site containing horsetail and sporadic clumps of short stature vegetation. It was classified as a young forest undergoing the stem-

exclusion phase of forest succession with a relatively uniform canopy dominated exclusively by black and interior spruce trees with maximum DBH and tree heights reaching 36cm and 26m respectively. A considerable number of standing dead trees were also present. Comparatively, plot 35 is a drier site classified as a mature forest consisting of a dominant canopy of lodgepole pine reaching 29m in height and 39cm DBH and a regenerating sub-canopy of subalpine fir. A few standing dead trees were present and short stature vegetation presence was minimal. ALS measured logs for each site are displayed as line segments overlain on a digitized version of the original CWD map for the $100m^2$ plots. All of the logs in plot 16, represented by figure 12a, are detected to some degree. CWD 1 is detected in the proper location however the orientation is shifted while CWD 2 is represented as two individual line segments, where the middle section of the log is not detected but the location and orientation are relatively accurate. Lastly, CWD 3 matches the ALS measured CWD however, it slightly overextends past the field measured endpoint. Plot 35, represented by Figure 12b, has three of four logs detected. ALS did not detect CWD 1 while CWD 2 and 3 were detected in the correct location but were shorter than the field measured logs. CWD 4 has the correct length; however it appears shifted from the field measured location by 50cm. Table 6 details the field measured attributes of all 28 logs and the corresponding attributes of those ones that were successfully detected.

Table 6. Comparison of field measured CWD attributes against diameter and length of ALS detected and measured CWD. Plots displayed in figure 12 are highlighted with a grey background.

Plot	ID	Average Diameter (cm)	Average Height Above Ground (cm)	Length (m)	Bark Class	Growth Class	Detection	Detected Diameter (cm)	Detected Length (m)
1	1	30.5	20	2.9	0	3	Missed	NA	NA
1	2	28.5	33	2.8	0	2	Detected	30	3.18

16	1	26.85	67.5	2.65	2	0	Detected	30	0.45
16	2	26.75	55	8.36	2	0	Detected	32	5.77
16	3	49.05	80	3.65	2	1	Detected	34	4.88
17	1	26.5	37	5.6	2	1	Missed	NA	NA
17	2	25.75	45	4.9	3	0	Detected	31	2.94
28	1	48.5	31.5	3.3	0	2	Missed	NA	NA
35	1	23.15	28	4.7	1	0	Missed	NA	NA
35	2	26.5	13.5	6.2	0	2	Detected	30	1.71
35	3	23.45	23	5.8	2	0	Detected	30	5.58
35	4	24.15	35.5	5	3	0	Detected	35	3.08
37	1	27.75	80	4.9	0	0	Detected	69	1.27
37	2	44.5	40.5	3.6	0	0	Missed	NA	NA
39	1	30.45	66.5	10.1	1	1	Detected	56	6.31
39	2	46.5	46.5	2.95	2	1	Detected	41	1.99
44	1	32.45	33	4.57	0	0	Detected	30	3.37
47	1	27.65	31	10	3	0	Detected	35	7.21
47	2	27	90	3.6	3	0	Detected	43	1.66
67	1	30.5	19	1.1	0	0	Missed	NA	NA
69	1	31.75	36.5	10.2	1	3	Missed	NA	NA
69	2	27.2	50	2.3	2	1	Missed	NA	NA
69	3	37.5	40	3.05	2	0	Detected	31	2.43
69	4	33	69.5	5.65	3	0	Detected	36	4.01
71	1	32.5	24.5	4.5	0	3	Detected	46	3.51
71	2	30	17.5	2.6	0	3	Missed	NA	NA
71	3	32.5	27	2.4	0	3	Missed	NA	NA
71	4	32.85	23	4.9	0	3	Detected	30	1.78

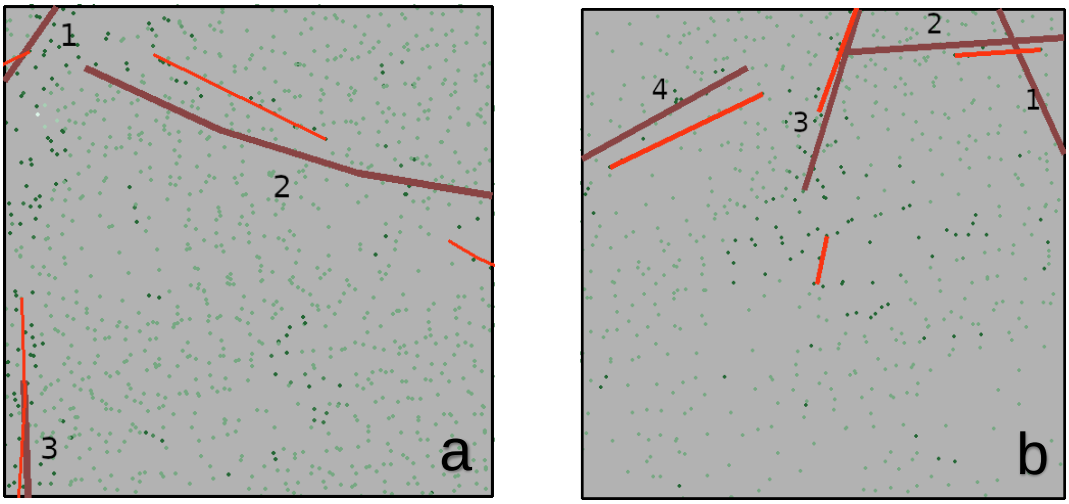

Figure 12. Digitized representations of the 10x10m plots 16 (a) and 35 (b). Detected linear segments are displayed in red, digitized measured logs are displayed in brown and ALS points <1m are displayed as green points.

4.3.2. Plot-level volume

The volume of each ALS detected CWD log was summed for each plot and compared to the field-measured summed CWD volumes (Figure 13). Results suggest that the relationship between the field and the ALS-derived volume was strong (R = 0.81, RMSE = 0.328 m^3). Figure 13 displays the ALS-measured CWD volume increasing in a linear pattern at the plot level with some variation from the field measured volume. One trend present is overestimation of CWD in plots containing lower volumes of CWD, with eight of the nine lowest-volume plots all seeing overestimated CWD volume. However, three of the four plots containing no CWD were also the plots with the lowest predicted volume using ALS. Minor underestimation of CWD at larger CWD volumes is also visible.

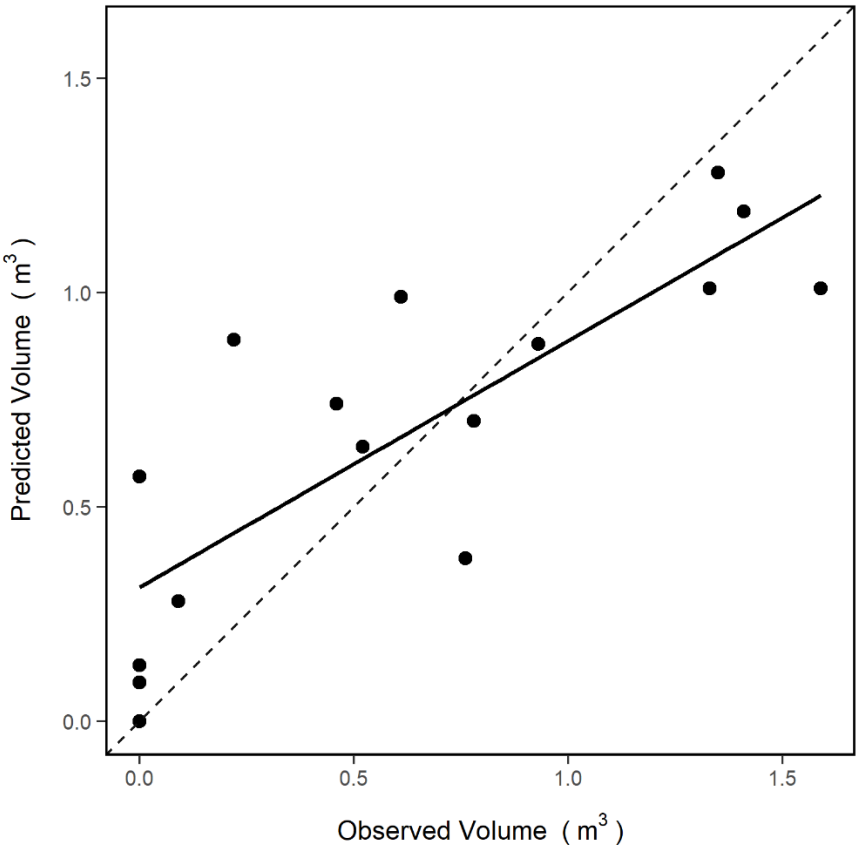

Figure 13. Regression comparison of ALS-predicted CWD volume versus observed field-measured CWD volume for 16 plots. Regression line displayed in black and 1:1 line displayed as a dashed line.

Assessment of the relationship between CWD detection and plot-level forest structure revealed the presence of some expected influences (Figure 14). Overall leaf-on vegetation presence, summarized by the percentage of ALS returns classified as ground, proved to be the most significant discriminating factor ($p = 0.015$) between detected and undetected logs with a higher percentage of ground points resulting in greater detection probability. A decrease in short stature vegetation presence, characterized by the number of sub-meter multi-return pulses, was also found to significantly increased the probability of CWD detection ($p = 0.039$). On average, plots

with a lower percentage of canopy cover had a better chance of detection; however, this relationship proved not statistically significant (p = 0.094). Height of the canopy, summarized by Lorey's mean height, presented no discernible trend over successful detection and was also proven insignificant (p = 0.901).

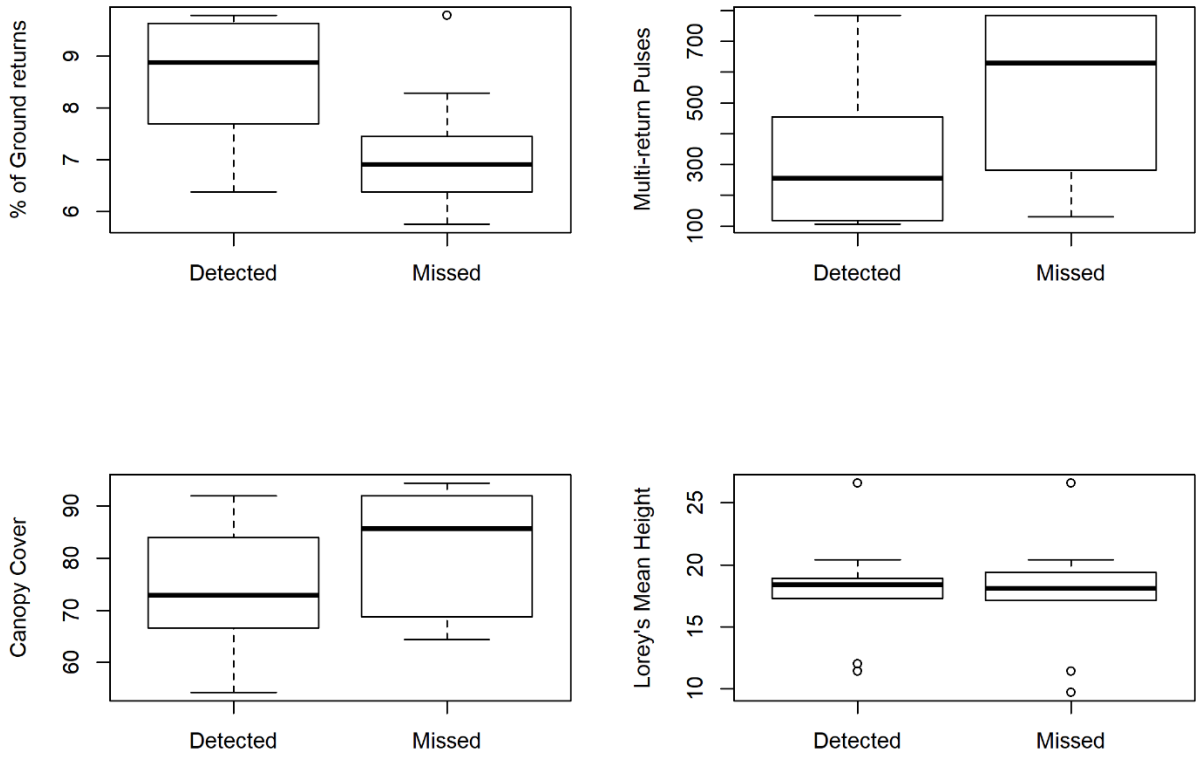

Figure 14. Influence of plot-level metrics over successful CWD detection (N= 15) and missed CWD (N=10).

4.3.3. Stand-level volume

Application of the methodology over a larger 2500 m^2 forested area consisting of four structurally different VRI polygons is displayed in figure 15. The map illustrates the four polygons located in the north-central region of the Deception Lake study area which was chosen due the structural gradient present within close proximity. The top left polygon of figure 15a is a

dry stand estimated at 110 years old with an average height of 21m and a canopy comprised of subalpine fir and lodgepole pine. The top right polygon is also an older stand estimated at 130 years old with an average height of 23 m, and the canopy is almost exclusively dominated by subalpine fir. The polygon located in the bottom right is a very old, late successional stage stand with a mixed canopy of subalpine fir and interior spruce with an estimated age of 165 years and an average height of 24 m. Lastly, the polygon in the bottom left is younger at 90 years, shorter with a 19 m average, and has a more homogenous canopy height dominated by lodgepole pine. The spatial distribution of CWD volume appears to vary both within and between these VRI units. The stand containing the greatest CWD volume is the oldest and tallest stand located in the bottom right with an average volume of 0.077 m^3 per pixel compared to 0.042 m^3 for the top right polygon and 0.040 m^3 for the top left polygon. The stand with the lowest CWD volume was the youngest and most homogenous stand located in the bottom left with an average volume of 0.022 m^3 per pixel. The polygon ALS-derived CWD estimation results suggest that older, more heterogenous stands have greater volumes of CWD. Regardless of stand type, large concentrations of CWD are present in clumps, with some linear features visible even at a five-meter pixel resolution. Figure 15b and 15c demonstrate that most of the detected linear points were transformed into CWD line segments in the highlighted area.

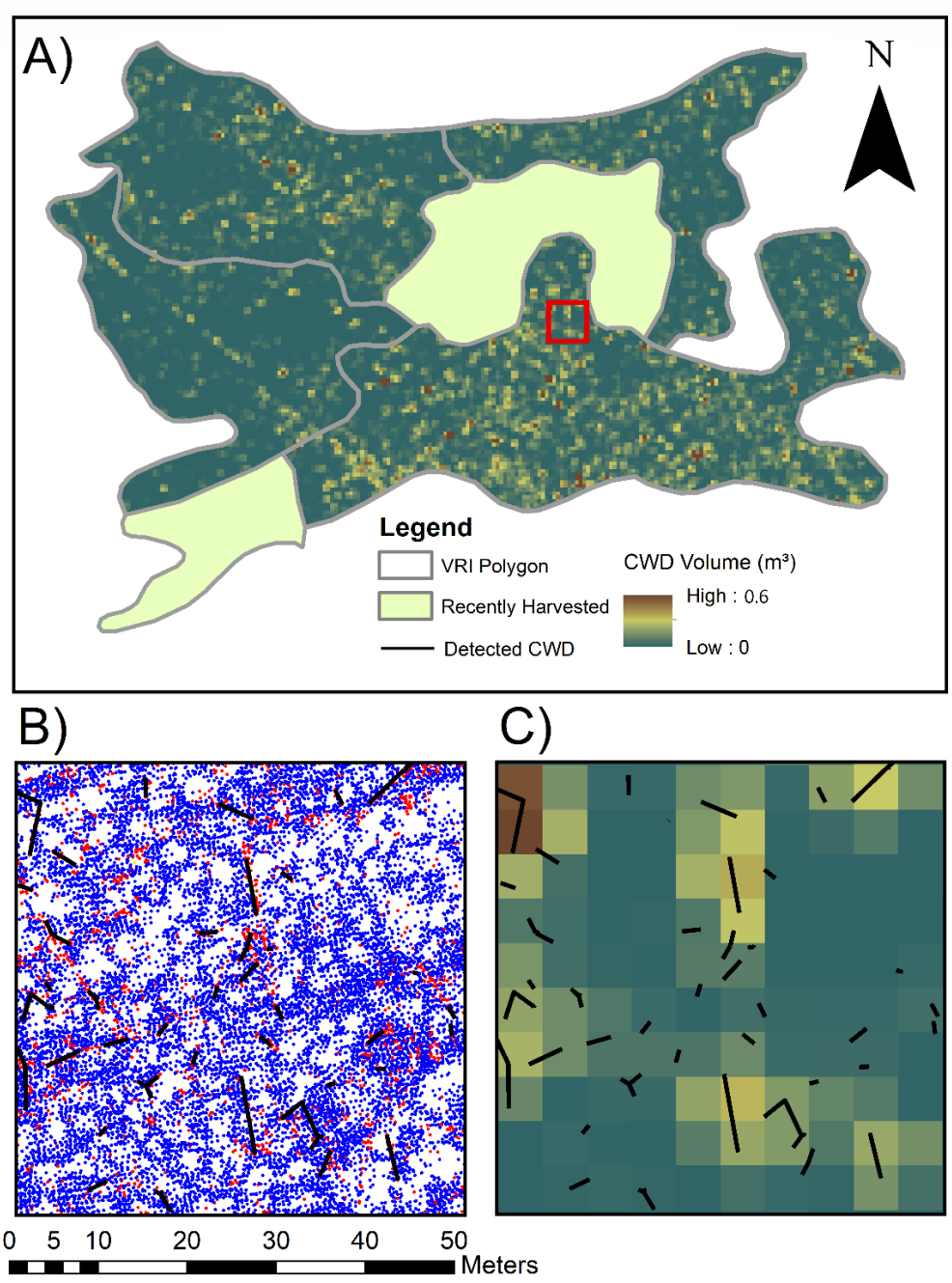

Figure 15. A) Predictive CWD volume map of VRI polygons. B) ALS point cloud displaying points identified as linear in red, all other points in blue, and detected logs in black. C) Inset of 5A, combining 5m raster cells and detected logs from 5B.

4.4. Discussion

In this chapter, I develop a methodology for isolating ALS returns associated with CWD greater than 30 cm in diameter and spatially transforming them into vectorized line segments with dimensional attributes extracted directly from the ALS point cloud. Additionally, a detailed analysis is conducted over a group of individual log and plot-level structural characteristics to identify any notable influences on detection rates. The developed methodology successfully detected 64% of CWD found in plots meeting the minimum density threshold of 7 pluses per meter. Successful detection was significantly influenced by log attributes as well as plot-level forest structural characteristics. Specifically, our analysis indicates that we can expect to accurately detect recently fallen CWD in natural forest stands containing relatively low understory vegetation cover. Despite the observed variance in detection rates, the overall plot-level CWD volume estimates generated by our methodology were strongly related to field-measured values. When applied at the stand level, the distribution of predicted CWD volume within and between stands followed the expected pattern of older and more vertically heterogeneous stands containing greater volumes of CWD.

4.4.1. Individual CWD assessment

Analysis of individual CWD attributes presented some unexpected findings, namely the insignificant influence of maximum or average diameter. Previous studies assessing CWD detection using ALS (Joyce et al., 2019; Nystrom et al., 2014) found CWD with greater diameter to be detected more frequently, however this effect was not observed in our study. A potential cause for this disagreement could be related to the minimum diameter considered for these studies having being lower. The minimum diameter of 30 cm may be an inflection point where

other attributes become more influential over detection; specifically, the average height above ground. Our results exemplify that an increase in average height above ground significantly increased detection rates ($p= 0.038$). Most undetected logs had a relatively low average height above the ground with some well below 30 cm, likely as a result of decomposition or being angled in a non-horizontal manner. Naturally, those logs which have a portion below 30cm are less likely to be detected with the implemented height filter. More elevated logs are less likely to be confused with low-lying shrubs or rocks, as there are fewer horizontal linear features that are not CWD as height above ground increases. These logs are also more likely to have recently fallen and less likely to be occluded by understory structure. Increasing CWD length also displayed a trend, suggesting that longer logs were more successfully detected, also noted by Joyce et al. (2019). However statistical testing for this study proved the relationship to be insignificant ($p=0.166$). Two notable influences towards this result were the longest CWD log in our study area not being detected (Table 3) combined with our smaller-than-desired sample size. Despite the length of this log, it was relatively low to the ground and is in a late stage of decay which suggests both these attributes are more influential than length.

The level of CWD decay, summarized in this chapter by bark and vegetation growth class, did demonstrate strong influence over CWD detection. CWD in later stages of decay were detected much less frequently then were logs with minimal decay. Recently fallen CWD, which would still have most of its bark and no vegetative growth, is more likely to fall on pre-existing understory structures such as boulders or older CWD and will therefore be more elevated, which has proved to aid in detection. In comparison, as CWD decomposes it becomes slowly engulfed by the organic layers of the forest floor, lowering average height above ground and making ALS detection less likely. Similar difficulty has been noted when attempting to detect late-stage

decomposition logs with ALS technology (Mucke et al. 2012). Additionally, these older logs are known to provide nutrients and become nurse logs for the growth of young saplings (Monleon, et al, 2002). Vegetation growing atop CWD would obscure the height and shape of the log represented in an ALS point cloud, further hindering detection probability. Although our methodology filters out multi-return pulses under two meters, considering them as shrubs, there is potential that vegetative growth atop old pieces of CWD would result in them being considered a shrub and filtered out of the analysis. Overall, the lower height and greater vegetative coverage of decomposed logs highlight why lower amounts of decayed CWD were detected.

4.4.2. Plot-level assessment

Analysis of plot-level metrics provided two stand-level attributes that proved influential in CWD detection: percentage of ALS returns classified as ground ($p = 0.015$) and the number of multi-return pulses under a meter ($p = 0.039$). Both metrics characterize vegetation cover with percent of ground returns representing overall vegetation cover including canopy, shrubs and herbs, while multi-return pulses only represent short statue vegetation. Both metrics provide a measure of physical obstructions that decrease the number of ALS returns that can interact with CWD. As such, plots with less vegetation cover are significantly more likely to result in successful CWD detection. Interestingly, Lorey's mean height which is a factor of tree height, had no influence at all, while the canopy cover metric did appear to inhibit CWD detection to some degree but not significantly ($p = 0.094$). This supports the finding that the percentage of ground returns is the most significant metric, as it is a combination of the multi-return and canopy cover metrics. These characteristics suggest that very dense canopies or understories may

inhibit successful CWD detection. At the plot level, the optimal forest structure for detection consists of a high percentage of ground returns, and an overall ALS pulse density greater than 7 pls/m^2.

While the above conditions are optimal for CWD detection, our CWD volume estimates predict plot level volume across a range of optimal and sub-optimal forest types. Examination of ALS measured plot volume against the field measurements revealed notable variation (RMSE = 0.328 m^3) but an overall strong correlation (R = 0.81). Compared to the field measured volume, the ALS derived methodology slightly overestimates plots with little or no CWD present. This is a result of small linear segments being generated from short-stature shrubs that are present in a linear orientation within the point cloud, a problem also noted by Lindberg et al. (2013) and Nystrom et al. (2014). Fortunately, it is rare for shrubs to grow in a linear fashion at length, leading to these false-positive line segments being short and resulting in only small overestimations. In plots with greater volumes of CWD, notable underestimation of CWD volume is present, which can be largely attributed to undetected CWD and detected line segments not representing the entire length of a log. Examples are present in Figure 12 where one large log is clearly detected in two separate line segments and other logs are not delineated to their complete length. Specifically, this is noticeable in plots with dense vegetation cover. Although our methodology attempts to connect nearby line segments, it is a purposely conservative approach to avoid the inclusion of non-CWD features being vectorized. From a volume perspective, the underestimation in length is partially offset by the liberal use of a single CWD height value as a proxy for diameter. A single height-based measurement assumes that all logs are perfectly horizontal, which is not the case in forest stands. However, based on the

majority of plot CWD volume still being underestimated, the use of a single diameter measurement does not appear to have a strong effect.

4.4.3. Stand-level assessment

Overall, the generated dimensions of length and height for each vectorized line vary and do not perfectly match the CWD they represent. However, total volume at the plot level seems to minimize this variation observed at the individual log level. As such, relative amounts and proportions of CWD volume estimated between plots are considerably accurate (R= 0.81) and present this methodology as a viable option for plot, stand and forest level quantification. This idea is reinforced when the methodology was applied over a larger area containing forest stands with known attributes to generate a predictive map of CWD volume. Within the map, older and more heterogeneous stands have a greater volume of CWD present which is in agreement with forest succession theory and current literature (Keeton et al., 2010; Stutz and Lang, 2017; Bilous et al, 2019). Taller stands generally have more CWD volume, but the tallest trees in a stand were not in the same location as the greatest CWD volume. Instead, the areas of highest CWD volume appear mainly in canopy gaps within these older stands, supporting the described influence of disturbances and gap dynamics on CWD accumulation (Tanhuanpää et al. 2015, Brazee et al., 2014). Longer logs also considerably increase the overall pixel volume, which is to be expected as longer logs are likely to have a great diameter and therefore greater volume. These are the most important CWD logs to identify as they will contribute the most to wildlife habitat and carbon stocks.

Chapter 5: Conclusion

5.1. Overview

The ability of ALS to characterize secondary forest structure was investigated over the course of this thesis. Secondary forest structure excludes the well-researched dominant canopy and focusses on the four lowest strata of forest structure, sub-canopy trees, understory vegetation, standing dead snags and CWD. The assessment was divided between the two secondary structure units that were lacking spatially quantifiable information, sub-canopy trees and CWD. In Chapter 3 a procedure is outlined with the flexibility to define the canopy and subcanopy at the stand level using relative position based on ALS-predicted HL. This procedure allowed for the removal of the canopy and generation of a suite of ALS metrics to describe attributes in the sub-canopy. Utilizing this removed-canopy methodology resulted in models with improved predictive capability for sub-canopy volume and basal area estimates over the retained canopy models. Utilizing the sub-canopy volume model, a predictive map was created across all forested landscapes in the Deception Lake study area that highlights locations and patterns of high sub-canopy volume across environmental gradients.

In Chapter 4 I investigated the capacity of ALS to detect and measure CWD directly from the point cloud. This was undertaken by creating an automated processing strategy which isolated ALS returns distributed in a linear pattern from short-stature vegetation and near-ground variability. The elevation of the registered CWD returns were then used to predict plot-level CWD volume. Results indicated the majority of CWD was detected and the proceeding volume estimates were strongly correlated with field-measured values. This processing strategy was then applied over a larger forested area to create a predictive map highlighting CWD volume gradients across multiple forest stands. Lastly, CWD detection rates are assessed against

measured individual, plot-level and stand-level attributes highlighting which attributes significantly increase detection rates.

5.2. Key findings

Assessment of sub-canopy tree structure revealed two important findings. First, ALS can be used to separate and distinguish sub-canopy components for the main canopy. Lorey's mean height can be reliably used as a baseline for a variable height threshold to distinguish between canopy and sub-canopy at the landscape level. This presents potential for further sub-canopy assessment to be conducted across a range of forest types with a uniform definition. Second, by applying this canopy threshold and using the sub-canopy model outlined in Chapter 3, volume of sub-canopy trees can be mapped with considerable accuracy ($r^2 = 0.88$, RMSE = 0.654 m^3) using common ALS metrics. Using the model to generate a predictive sub-canopy maps allows for inventory of the sub-canopy which is important for guiding land use decisions around locations for alternative harvesting practices, wildfire fuel load management and habitat retention.

The CWD portion of the investigation highlighted three key findings. First, ALS returns associated with CWD can be successfully spatially isolated and mapped directly from an ALS point cloud utilizing the processing strategy outlined in Chapter 4. This strategy transforms selected point could returns into measurable polyline vectors. Second, average return height of detected CWD points may be used as a substitute for a diameter measurement to generate reliable plot-level and stand-level CWD volume. Third, detection of CWD using ALS is significantly influenced by individual log as well as plot-level attributes. More decayed pieces of CWD were detected considerably less often while CWD with a high average height above ground were significantly more often ($p = 0.038$). Plots with a higher percentage of ground

returns and a lower percentage of multi-hit returns proved to increase detection rates. These plot level metrics can be used to determine forest stands where the processing strategy can be applied and most effective.

5.3. Implications

The results presented in Chapter 3 have important implications for forest mangers who have acquired, or are planning to obtain, ALS data. If ALS data exists, it would be possible to implement the methodology outlined in this thesis as it consists of commonly used and easily generated ALS metrics to create an inventory of sub-canopy forest structure previously only obtainable though field measurements. This inventory can be used by land managers for a number of purposes including selecting candidate locations for selective logging to preserve mid-term timber opportunities, fire susceptibility and carbon sequestration modelling, and wildlife habitat values. The sub-canopy approach produces new descriptive metrics of forest structure that can aid in updating and refining classification system within British Columbia including site series mapping, succession and structural stages of forested landscapes as outlined in the BC Government Field Manual for Describing Terrestrial Ecosystems (Province of British Columbia, 2015). Repeated acquisition of ALS over time coupled with sub-canopy inventory generation could highlight changes in the subcanopy and present a spatial representation of forest growth and successional patterns over time. Lastly, future studies focusing on sub-canopy trees can use this inventory to located optimal sites containing the desired quantity of sub-canopy trees.

Given the importance of CWD for carbon modelling, detecting and mapping CWD will highlight regions with increased levels of carbon storage and allows for a spatial representation of this

import carbon sink. Production of CWD maps can aid forest professionals in locating and quantifying CWD over a range of natural forest stands to sponsor a more well-rounded quantification of carbon levels, wildlife habitat and fuel loading in the terrestrial biosphere. Obtaining these more accurate carbon estimates is critical for land managers given the recent emphasis on reporting stored carbon levels (Boisvenue et al., 2016; Ford and Keeton, 2017). Quantifying CWD volume for a stand can also be integrated into the conventional polygon based VRI system as an attribute to enhance reliability and descriptive capability of current VRI polygons.

5.4. Limitations

The canopy removal using Lorey's mean height outlined in Chapter 3 proved to be successful, however some limitations need to be considered. Even once the canopy was removed structural elements of canopy trees such as stems and branches are still present in the removed canopy point cloud. Although this suggests the removed canopy point cloud is not a direct representation of sub-canopy trees, the models developed in this study still appear to provide as a reliable proxy. Another limitation is the smaller-than-desired number of sample sites and was constrained to forest types typical of only a limited set of biogeoclimatic units. Characteristics of tree species and forest structure in other regions may have differing opacity to canopy penetration with ALS that could affect predictive capability. The predictive capability amongst other forest types must be further explored and validated to support broader application of this approach.

Limitations surrounding Chapter 4 include the relatively small number of CWD pieces measured. The structural sampling procedure implemented for plot selection provided a diverse range of forest structure however, many of these contained little or no CWD, contributing to the

low number. Additionally, a minimum point density of 7 points/m^2 between 0 and 1m was required for optimal detection. Although this is within the range of modern operational-level ALS, dense canopy coverage can severely reduce the point density at ground level, as it did for twelve of my plots. Volume estimates generated in this study only account for logs greater than 30cm diameter. While these logs contribute 79% of total CWD volume and are more influential for carbon estimates and wildlife studies, there is a notable amount under 30cm diameter that is excluded. Lastly, this methodology expands CWD detection into naturally forested areas with moderate canopy cover, but predictive was shown to still be restricted by increasing dense canopy coverage.

5.5. Future research

The methodologies presented within this thesis provide a starting point for the development of a detailed sub-canopy forest inventory to complement and enhance existing forest inventories. The primary direction for future research should focus on testing the applicability of the sub-canopy models in the other biogeoclimatic zones of British Columbia and beyond. If successful, a province-wide inventory of sub-canopy structure could provide a holistic representation of forest structure and bolster the current provincial inventory (Bourgeois et al., 2018).

Large-scale application of any ALS methodology requires expanded data acquisition. To limit costs, research into point cloud thinning is suggested to assess if similar results can be achieved at lower point cloud densities, a strategy commonly used in conjunction with other ALS attributes (Wilkes et al., 2015; Hamraz et al., 2017). Additionally, results from Chapter 3 are indicative of a relationship between sub-canopy tree volume and topographic variables.

Characterizing this relationship could provide a stronger connection between sub-canopy volume and productivity patterns.

The successful delineation of CWD presented in Chapter 4 presents an opportunity for expansion into different ecosystems. Specifically, the methodology has potential to be adapted to aquatic environments such as rivers and streams where CWD is a critical component of ecosystem heterogeneity and fish habitat (Gippel, 1995; Mossop and Bradford, 2004). Stream environments generally contain less canopy coverage and the results from chapter 4 indicate these areas would likely result in more accurate detection. The relative lack of ground-level vegetation in stream environments also presents an opportunity to integrate intensity value filtering into the CWD processing strategy. Woody material would return greater intensity compared to water (Hooshyar et al., 2015) and has previously been used to separate water returns from terrestrial objects (Höfle et al., 2009) This would further isolate CWD related returns and improve upon the delineation presented in Chapter 4, although intensity calibration issues should be considered (Ahokas et al., 2006; Boyd and Hill, 2007).

Further research into the spatial distribution of CWD volume may be useful in generating habitat suitability indices for the multitude of species reliant on CWD (Jonsson et al., 2005). Implementing the CWD detection methodology also presents potential work investigating the integration of CWD thresholds into forest classification systems. CWD is a common indicator of old-growth ecosystems (Feller, 2003; Keren and Diaci, 2018) and the quantification of CWD presented in Chapter 4 could be used to establish thresholds for classification of high-value old-growth forest stands.

Lastly, opportunities exist for future studies to combine the products of Chapter 3 and Chapter 4 to characterize the relationship between sub-canopy attributes. Comparing sub-canopy tree

volume to understory vegetation coverage and CWD volume could yield further insights into overall forest structure, development and growth patterns (Acker et al., 2017; Kumar et al., 2018). This integrated overview of forested landscapes would provide valuable details to forest and land mangers to optimize resources allocation. Future research into sub-canopy forest structure should focus on integrating the methodologies and products presented in this thesis into and integrated inventory of forest structure.

References

Abalharth, M. (2013). Using LiDAR to detect in-stream wood: a scaled approach. University of British Columbia

Acker, S., Kertis, J., & Pabst, R. (2017). Tree regeneration, understory development, and biomass dynamics following wildfire in a mountain hemlock (Tsuga mertensiana) forest. *Forest Ecology and Management*, 384, 72-82.

Agca, M., Popescu, S.C., & Harper, C.W. (2011). Deriving forest canopy fuel parameters for loblolly pine forests in eastern Texas. *Canadian Journal of Forest Research*, 41(8), 1618-1625.

Agee, J.K. (1996). The influence of forest structure on fire behavior.17th forest vegetation management conference, Redding, CA, 16–18 February 1996: 52–68.

Ahokas, E., Kaasalainen, S., Hyyppä, J., & Suomalainen, J. (2006). Calibration of the optech ALTM 3100 laser scanner intensity data using brightness targets. *The International Archives of the Photogrammetry, Remote Sensing and Spatial Information Sciences*, 34, 3-6.

Amoroso, M.M., Coates, K.D. & Astrup, R. (2013). Stand recovery and self-organization following large-scale mountain pine beetle induced canopy mortality in northern forests. *Forest Ecology and Management*, 310, 300 – 311.

Angelstam, P. (1996). The ghost of forest past — natural disturbance regimes as a basis for reconstruction of biologically diverse forests in Europe. *Conservation of Faunal Diversity in Forested Landscapes (Conservation Biology)*, 6.

Aponte, C., Tolhurst, K., & Bennett, L. (2014). Repeated prescribed fires decrease stocks and change attributes of coarse woody debris in a temperate eucalypt forest. *Ecological Applications*, 24(5), 976-989.

Babcock, C., Matney, J. Finley, A.O, Weiskittel, A. & Cook, B.D. (2013). Multivariate Spatial Regression Models for Predicting Individual Tree Structure Variables Using LiDAR

Data. *IEEE Journal of Selected Topics in Applied Earth Observations and Remote Sensing*, 6(1): 6-14.

Banner, A., MacKenzie, W., Haeussler, S., Thomson, S., Pojar, J., & Trowbridge, R. (1993). A field guide to site identification and interpretation for the Prince Rupert Forest Region. B.C. Ministry of Forest Resources Branch, Victoria, B.C., *Land Management Handbook*, No. 26.

Béland, M., Baldocchi, D., Widlowski, J., Fournier, R., & Verstraete, M. (2014). On seeing the wood from the leaves and the role of voxel size in determining leaf area distribution of forests with terrestrial LiDAR. *Agricultural and Forest Meteorology*, 184, 82-97.

Blanchard, S., Jakubowski, M., & Kelly, M. (2011). Object-based image analysis of downed logs in disturbed forested landscapes using lidar. *Remote Sensing*, 3(11), 2420-2439.

Bohn, F., & Huth, A. (2017). The importance of forest structure to biodiversity–productivity relationships. *Royal Society Open Science*, 4(1), 160521.

Bolton, D., Coops, N., & Wulder, M. (2013). Investigating the agreement between global canopy height maps and airborne Lidar derived height estimates over Canada. *Canadian Journal of Remote Sensing*, 39(1), S139-S151.

Bolton, D., Coops, N., Hermosilla, T., Wulder, M., & White, J. (2017). Assessing variability in post-fire forest structure along gradients of productivity in the Canadian boreal using multi-source remote sensing. *Journal of Biogeography*, 44(6), 1294-1305.

Bourgeois, W. (2004). Future forest management in British Columbia: A proposed vision, goals, and forest management framework. *Journal of Ecosystems and Management*, 4(1).

Bourgeois, C., Binkley, W., Lemay, C., Moss, V., & Reynolds, I. (2018). British Columbia Forest Inventory Review Panel Technical Background Report. Prepared for the Office of the Chief Forester Division, British Columbia Ministry of Forests, Lands, Natural Resource Operations and Rural Development.

Bouvier, M., Durrieu, S., Fournier, A., & Renaud, J.-P. (2015). Generalizing predictive models of forest inventory attributes using an area-based approach with airborne LiDAR data. *Remote Sensing of Environment*, 156, 322–334.

Boyd, D., & Hill, R. (2007). Spatio-Temporal Dynamics of Forest Response to ENSO Drought (STEED). Validation of airbourne LiDAR intensity values from a forested landscape using HYMAP data: preliminary analysis.

British Columbia Ministry of Forests and Range. Silviculture Program Statistics. 2018. Available online: https://www2.gov.bc.ca/gov/content/industry/forestry/managing-our-forest-resources/silviculture/silviculture-statistics

Brazee, N., Lindner, D., D'Amato, A., Fraver, S., Forrester, J., & Mladenoff, D. (2014). Disturbance and diversity of wood-inhabiting fungi: Effects of canopy gaps and downed woody debris. *Biodiversity and Conservation*, 23(9), 2155-2172.

Brubacker, K.M. Myers, W.L., Drohan, P.J., Miller, D.A., & Boyer, E.W. (2013). The Use of LiDAR Terrain Data in Characterizing Surface Roughness and Microtopography. *Applied and Environmental Soil Science*, 2013, 13. https://doi.org/10.1155/2013/891534

Brunialti, G., Frati, L., Aleffi, M., Marignani, M., Rosati, L., Burrascano, S., & Ravera, S. (2010). Lichens and bryophytes as indicators of old-growth features in Mediterranean forests. *Plant Biosystems*, 144(1), 221-233.

Buckley. A.J. (1992) Fire behaviour and fuel reduction burning: Bemm River wildfire, *Australian Forestry*, 55, 135-147.

Bunnell, F.L. 1995. Forest-Dwelling Vertebrate Faunas and Natural Fire Regimes in British Columbia: Patterns and Implications for Conservation. *Conservation Biology*, 9(3), 636-644.

Bunnell, F.L., Dunsworth, G.B., Huggard, D.H., and Kremsater, L.L. (2009). Forestry and Biodiversity: Learning How to Sustain Biodiversity in Managed Forests. Edited by F.L. Bunnell and G.B. Dunsworth. University of British Columbia Press, Vancouver, BC. pp. 5–16.

Bunnell, F., & Houde, I. (2010). Down wood and biodiversity — implications to forest practices. *Environmental Reviews*, 18, 397-421.

Campbell M.J., Dennison, P.E., Hudak, A.T. Parham, L.M., & Butler, B.W. (2018). Quantifying understory vegetation density using small-footprint airborne lidar. *Remote Sensing of Environment*, 215, 330-342.

Campbell, J. L., Green, M.B., Yanai, R.D., Woodall, C.W. Fraver, S., Harmon, M.E., Hatfield, M.A. Barnett, C.J., See, C. R. & Domke, G.M. (2019). Estimating uncertainty in the volume and carbon storage of downed coarse woody debris. *Ecological Applications,* 29(2), e01844. 10.1002/eap.1844

Cansler, C., Swanson, M., Furniss, T., Larson, A., & Lutz, J. (2019). Fuel dynamics after reintroduced fire in an old-growth Sierra Nevada mixed-conifer forest. *Fire Ecology,* 15(1), 1-17.

Caviedes, J., & Ibarra, J. (2017). Influence of Anthropogenic Disturbances on Stand Structural Complexity in Andean Temperate Forests: Implications for Managing Key Habitat for Biodiversity, *PLOS ONE*, 12(1), e0169450.

Charchuk, C. & Bayne, E.M. (2018) Avian community response to understory protection harvesting in the boreal forest of Alberta, Canada. *Forest Ecology and Management,* 407, 9-15.

Chasmer, L., Hopkinson, C. & Treitz, P. (2006). Investigating laser pulse penetration through a conifer canopy by integrating airborne and terrestrial lidar. *Canadian Journal of Remote Sensing*, 32(2), 116-125.

Chirici, G., Winters, S., R.E McRoberts. (2011). National Forest Inventories: Contributions to Forest Biodiversity Assessments. *Springer*.

Choi, S., Lee, J., Han, S., Kim, S., & Son, Y. (2015). Estimating Wildfire Fuel Load of Coarse Woody Debris using National Forest Inventory Data in South Korea. *Journal of Climate Change Research*, 6(3), 185.

Clark, M.L., Clark, D.B., & Roberts, D.A. (2004). Small-footprint lidar estimation of sub-canopy elevation and tree height in a tropical rain forest landscape. *Remote Sensing of Environment*, 91, 68-89.

Coates, K.D., DeLong, C., Burton, P.J. & Sachs, D.L. (2006). Abundance of Secondary Structure in Lodgepole Pine Stands Affected by the Mountain Pine Beetle. *Report for the Chief Forester*, August, 2006. 17 pp.

Coates, K. D. & Sachs, D.L. (2012). Current State of Knowledge Regarding Secondary Structure in Mountain Pine Beetle Impacted Landscapes. *MPB Impacted Stands Assessment Project*.

Connell, J.H., Lowman, M.D. & Noble I.R. (1997). Subcanopy gaps in temperate and tropical forests. *Australian Journal of Ecology*, 22, 163 – 168.

Coops, N.C., Hilker,T., Wulder, M.A., St-Onge, B., Newnham, G. Siggins, A & Trofymow, J.A. (2007). Estimating canopy structure of Douglas-fir forest stands from discrete-return LiDAR. *Trees*, 21, 295

Coops, N.C., Tompalski, P., Nijland, W., Rickbeil, G.J.M., Nielsen, S.E., Bater, C.W. & Stadt, J.J. (2016). A forest structure habitat index based on airborne laser scanning data. *Ecological Indicators*, 67, 346 – 357.

Del Río, M., Pretzsch, H., Alberdi, I., Bielak, K., *et al*. (2016). Characterization of the structure, dynamics, and productivity of mixed-species stands: review and perspectives. *European Journal of Forest Research,* 135, 23-49.

Dupuy, J., & Chazdon, R. (2008). Interacting effects of canopy gap, understory vegetation and leaf litter on tree seedling recruitment and composition in tropical secondary forests. *Forest Ecology and Management, 255*(11), 3716-3725.

ESRI (2019). ArcGIS Desktop: Release 10.5 Redlands, CA: Environmental Systems Research Institute.

Falkowski, M.J., Evans, J.S., Martinuzzi, S, Gessler, P.E. & Hudak, A.T. (2009). Characterizing forest succession with lidar data: An evaluation for the Inland Northwest, USA. *Remote sensing of the Environment*, 11, 946-956.

Farnell, I., Elkin, C., Lilles, E. Roberts, A-M., & Venter, M. (2020). The effects of variable retention forestry on coarse woody debris dynamics and concomitant impacts on American marten habitat after 27 years. *Canadian Journal of Forest Research,* Accepted for publication: June 9th , 2020.

Feller, M. (2003). Coarse woody debris in the old-growth forests of British Columbia. *Environmental Reviews*, 11(S1), S135-S157.

Ferster, C., Coops, N.C. & Trofymow, J.A. (2009). Aboveground large tree mass estimation in a coastal forest in British Columbia using plot-level metrics and individual tree detection from LiDAR. *Canadian Journal of Remote Sensing*, 35, 270-275.

Ford, S., & Keeton, W. (2017). Enhanced carbon storage through management for old-growth characteristics in northern hardwood-conifer forests. *Ecosphere*, 8(4).

Franklin, S., Maudie, A.J. & Lavigne, M. (2001). Using spatial co-occurrence texture to increase forest structure and species composition classification accuracy. *Photogrammetric Engineering and Remote Sensing*, 67, 849-855.

Franklin, J., Spies, T., Pelt, R., Carey, A., Thornburgh, D., Berg, D., Lindenmayer, D.B., Harmon, M.E., Keeton, W.S., Shaw, D.C., Bible, K. & Chen, J. (2002). Disturbances and structural development of natural forest ecosystems with silvicultural implications, using Douglas-fir forests as an example. *Forest Ecology and Management*, 155(1-3), 399-423.

Gao, T., Hedblom, M., Emilsson, T., & Nielsen, A. (2014). The role of forest stand structure as biodiversity indicator. *Forest Ecology and Management*, 330, 82-93.

Goodwin, N. R., Coops, N.C., Bater, C., & Gergel, S.E. 2007. Assessment of sub-canopy structure in a complex coniferous forest. *In Proceedings of the ISPR Workshop "Laser Scanning 2007 and SilviLaser 2007*", Espoo, September 12-14, 2007, Finland (Vol. 36, pp. 169-172).

Gough, C., Vogel, C., Kazanski, C., Nagel, L., Flower, C., & Curtis, P. (2007). Coarse woody debris and the carbon balance of a north temperate forest. *Forest Ecology and Management*, 244(1-3), 60-67.

Grote, R., Kiese, R., Grunwald, T., Ourcival, J.M., Granier, A. (2011). Modelling forest carbon balances considering tree mortality and removal. *Agriculture For Meteorology*, 51, 179-190.

Hall, S.A., Burke, I.C., Box, D.O., Kaufmann, M.R., & Stoker, J.M. (2005). Estimating stand structure using discrete-return lidar: an example from low density fire prone ponderosa pine forests. *Forest Ecology and Management*, 208, 189-209.

Hall, R., Skakun, R., Arsenault, E., & Case, B. (2006). Modeling forest stand structure attributes using Landsat ETM+ data: Application to mapping of aboveground biomass and stand volume. *Forest Ecology and Management*, 225(1-3), 378-390.

Halofsky, J.E., Peterson, D.L. & Harvey, B.J. (2020). Changing wildfire, changing forests: the effects of climate change on fire regimes and vegetation in the Pacific Northwest, USA. *Fire Ecology*, 16, 4.

Hamann, A., & Wang, T. (2006). Potential effects of climate change on ecosystem and tree species distribution in British Columbia. *Ecology*, 87(11), 2773-2786.

Hamraz, H., Contreras, M.A., & Zhang, J. (2017). Forest understory trees can be segmented accurately within sufficiently dense airborne laser scanning point clouds. Scientific Reports 7: 6770.

Hann, D. (2011). Revised Volume and Taper Equations for Six Major Conifer Species in Southwest Oregon. Oregon State University, Corvallis, Oregon.

Harmon, M.E., Franklin, J.F., Swanson, F.J., Sollins, P., Gregory, S.V., Lattin, J.D., Anderson, N.H., Cline, S.P., Aumen, N.G., Sedell, J.R., Lienkaemper, G.W., Cro-mack, K., & Cummins, K.W. (1986). Ecology of coarse woody debris in temperate ecosystems. *Advances in Ecological Research*, 15, 133–302. https://doi.org/10.1016/S0065-2504(03)34002-4

Harmon, M., & Franklin, J. (1989). Tree seedlings on logs in Picea-Tsuga forests of Oregon and Washington. *Ecology*, 70(1), 48-59.

Harmon, M.E., Fasth, B.G., Yatskov, M., Kastendick, D., Rock, J., & Woodall, C.W. (2020). Release of coarse woody detritus-related carbon: a synthesis across forest biomes. *Carbon Balance Management*, 15, 1. https://doi.org/10.1186/s13021-019-0136-6

Hawkins, C.D.B., Dhar, A., & Balliet, N.A. (2013). Radial growth of residual overstory trees and understory saplings after mountain pine beetle attack in central British Columbia. *Forest Ecology and Management*, 310, 348-356.

Helms, J.A. (1979). Positive effects of prescribed burning on wildfire intensities. *Fire Management Notes*, 40, l0-13.

Hermosilla, T., Ruiz, L., Kazakova, A., Coops, N., & Moskal, L. (2014). Estimation of forest structure and canopy fuel parameters from small-footprint full-waveform LiDAR data. *International Journal of Wildland Fire*, 23(2), 224.

Hilker, T., Frazer, G., Coops, N., Wulder, M., Newnham, G., Stewart, J., Culvenor, D. (2013). Prediction of Wood Fiber Attributes from LiDAR-Derived Forest Canopy Indicators. *Forest Science*, 59(2), 231-242.

Hill, R. & Broughton, R. (2009). Mapping the understory of deciduous woodland from leaf-on and leaf-off airborne LiDAR data: A case study in lowland Britain. *Journal of Photogrammetry and Remote Sensing*, 64(2), 223-233.

Hillman, S., Wallace, L., Reinke, K., Hally, B., Jones, S., & Saldias, D. (2019). A Method for Validating the Structural Completeness of Understory Vegetation Models Captured with 3D Remote Sensing. *Remote Sensing*, 11(18), 2118.

Höfle, B., Vetter, M., Pfeifer, N., Mandlburger, G., & Stötter, J. (2009). Water surface mapping from airborne laser scanning using signal intensity and elevation data. *Earth Surface Processes and Landforms*, 34(12), 1635-1649.

Holling, C.S. (1992). Cross-Scale Morphology, Geometry, and Dynamics of Ecosystems. *Ecological Monographs*, 62(4), 447-502.

Holmgren, J. (2004). Prediction of tree height, basal area and stem volume in forest stands using airborne laser scanning. *Scandanavian Journal of Forest Research*, 19(6), 543-553.

Hooshyar, M., Kim, S., Wang, D., & Medeiros, S. (2015). Wet channel network extraction by integrating LiDAR intensity and elevation data. *Water Resources Research,* 51(12), 10029-10046.

Horn, S. (1975). Forest Succession. *Scientific American*, 232(5), 90-101.

Husch, B., Miller, C.I. & Beers, T.W. (1982). Forest mensuration, 3rd ed. John Wiley and Sons, New York. 402 p.

Hunter, M. L. (1999). Maintaining biodiversity in forest ecosystems. *Cambridge University Press*, Cambridge, United Kingdom.

Hyyppa, J., Kelle, O., Lehikoinen, M., & Inkinen, M. (2001). A segmentation-based method to retrieve stem volume estimates from 3-D tree height models produced by laser scanners. *IEEE Transactions on Geoscience and Remote Sensing*, 39(5), 969-975.

Inoue, T., Nagai, S., Yamashita, S., Fadaei, H., Ishll, R., Okabe, K., *et al*. (2014). Unmanned aerial survey of fallen trees in a deciduous broadleaved forest in eastern Japan. *PLoS ONE*, 9, e109881.

Irwin, J. R. (2018). Quantification of Understory Fuels in the Superior National Forest Using Lidar Data (Doctoral dissertation, Geography Department, South Dakota State University).

Isenburg, M. (2014). LAStools — efficient tools for LiDAR processing (Version 141017, Academic) obtained from http://rapidlasso.com/LAStools

Jarron, L., Coops, N., MacKenzie, W., Tompalski, P., & Dykstra, P. (2020). Detection of sub-canopy forest structure using airborne LiDAR. *Remote Sensing of Environment*, 244, 111770.

Jakubowksi, M. K., Guo, Q., Collins, B., Stephens, S. & Kelly, M. (2013). Predicting surface fuel models and fuel metrics using lidar and CIR imagery in a dense mixed conifer forest. *Photogrammetric Engineering and Remote Sensing*, 79(1), 37-49.

Jonsson, B., Kruys, N., & Ranius, T. (2005). Ecology of species living on dead wood - Lessons for dead wood management. *Silva Fennica*, 39(2), 289-309.

Jönsson, M., & Jonsson, B. (2007). Assessing coarse woody debris in Swedish woodland key habitats: Implications for conservation and management. *Forest Ecology and Management*, 242(2-3), 363-373.

Jordan, G., Ducey, M., & Gove, J. (2004). Comparing lines-intersect, fixed-area, and point relascope sampling for dead and downed coarse woody material in a managed northern hardwood forest. *Canadian Journal of Forest Research*, 34(8), 1766-1775.

Keane, R.E., (2014). Wildland Fuel Fundamentals and Applications. *Springer*.

Keeton, W., Chernyavskyy, M., Gratzer, G., Main-Knorn, M., Shpylchak, M., & Bihun, Y. (2010). Structural characteristics and aboveground biomass of old-growth spruce–fir stands in the eastern Carpathian mountains, Ukraine. *Plant Biosystems*, 144(1), 148-159.

Keisker, D. (2000). Types of Wildlife Trees and Coarse Woody Debris Required by Wildlife of North-Central British Columbia. British Columbia, Ministry of Forests Research Program.

Kennedy, P., & Quinn, T. (2001). Understory plant establishment on old-growth stumps and the forest floor in western Washington. *Forest Ecology and Management*, 154(1-2), 193-200.

Keren, S., & Diaci, J. (2018). Comparing the Quantity and Structure of Deadwood in Selection Managed and Old-Growth Forests in South-East Europe. *Forests*, 9(2), 76.

Kimberley, M., Beets, P., & Paul, T. (2019). Comparison of measured and modelled change in coarse woody debris carbon stocks in New Zealand's natural forest. *Forest Ecology and Management*, 434, 18-28.

Kirchmeier-Young, M.C., Gillett, N.P., Zwiers, F.W., Cannon, A.J., & Anslow, F.S. (2019). Attribution of the Influence of Human-Induced Climate Change on an Extreme Fire Season. *Earth's Future*, 7(1), 2-10.

Korpela, I., Hovi, A., & Morsdorf, F. (2012). Understory trees in airborne LiDAR data — selective mapping due to transmission losses and echo-triggering mechanisms. *Remote Sensing of the Environment*, 119, 92–104.

Král, K., Janík, D., Vrška, T., Adam, D., Hort, L., Unar., P & P. Šamonil. (2010). Local variability of stand structural features in beech dominated natural forests of Central Europe: Implications for sampling. *Forest Ecology and Management,* 260(12), 2196-2203.

Kramer, H., Collins, B.M., Kelly, M., & Stephens, S.L. (2014). Quantifying Ladder Fuels: A New Approach Using LiDAR. *Forests,* 5, 1432-1453.

Kramer, H., Collins, B.M., Lake, F. K., Jakubowski, M., Stephens, S. L. & Kelly, M. (2016). Estimating Ladder Fuels: A New Approach Combining Field Photography with LiDAR. *Remote Sensing*, 8.

Krebs, M., Reeves, M., & Baggett, L. (2019). Predicting understory vegetation structure in selected western forests of the United States using FIA inventory data. *Forest Ecology and Management*, 448, 509-527.

Kuhn, M. (2008). Building Predictive Models in R Using the caret Package. *Journal of Statistical Software,* 28(5), 1 – 26.

Kumar, P., Chen, H., Thomas, S., & Shahi, C. (2018). Linking resource availability and heterogeneity to understory species diversity through succession in boreal forest of Canada. (F. Gilliam, Ed.) *Journal of Ecology*, 106(3), 1266-1276.

Landers, L. J. & Boyer, W.D. (1999). An old-growth definition for upland longleaf and south Florida slash pine forests, woodlands, and savannas. Gen. Tech. Rep. SRS-29. Asheville, NC: U.S. Department of Agriculture, Forest Service, Southern Research Station.

Larson, A.J., Lutz, J.A., Gersonde, R.F., Franklin., J.F., & Hietpas, F.F. (2008). Potential site productivity influences the rate of forest structural development. Ecological Indicators, 18(4), 899 – 910. https://doi.org/10.1890/07-1191.1

Latifi, H., Heurich, M., Hartig, F., Müller, J., Krzystek, P., Jehl, H., & Dech, S. (2016). Estimating over- and understory canopy density of temperate mixed stands by airborne LiDAR data. *Forestry: An International Journal of Forest Research*, 89(1), 69–81.

Lelli, C., Bruun, H., Chiarucci, A., Donati, D., Frascaroli, F., Fritz, Ö., Heilmann-Clausen, J. (2019). Biodiversity response to forest structure and management: Comparing species

richness, conservation relevant species and functional diversity as metrics in forest conservation. *Forest Ecology and Management*, 432, 707-717.

Leemans, R. (1991). Canopy gaps and establishment patterns of spruce (Picea abies (L.) Karst.) in two old-growth coniferous forests in central Sweden. *Vegetation*, 93 (2), 157-165.

Lefsky, M.A., Cohen, W.B., Parker, G.G., & Harding, D.J. (2002). Lidar remote sensing for ecosystem studies. *Bioscience*, 52, 19.

Lertzman, K., Fall, J., & Dorner, B. (1998). Three kinds of heterogeneity in fire regimes: at the crossroads of fire history and landscape ecology. *Northwest Science*, 72, 4-23.

Liang, X., Kankare, V., Hyyppä, J., Wang, Y., Kukko, A., Haggrén, H., Vastaranta, M. (2016,). Terrestrial laser scanning in forest inventories. ISPRS Journal of *Photogrammetry and Remote Sensing*, 115, 63-77.

Lim, K., Treitz, P., Wulder, M.A., St-Onge, B., & Flood, M. (2003). LiDAR remote sensing of forest structure. *Progress in Physical Geography*, 27, 88-106.

Limberger, F., & Oliveira, M. (2015). Real-time detection of planar regions in unorganized point clouds. *Pattern Recognition*, 48(6), 2043-2053.

Lindberg, E., Hollaus, M., Mücke, W., Fransson, J., & Pfeifer, N. (2013). Detection of lying tree stems from airborne laser scanning data using a line template matching algorithm. *ISPRS Annals of the Photogrammetry, Remote Sensing and Spatial Information Sciences*, 2,169-174.

Lu, D. (2005). Aboveground biomass estimation using Landsat TM data in the Brazilian Amazon. *International Journal of Remote Sensing*, 26(12), 2509-2525.

Lutes, D., & Keane, R. (2006). FIREMON: Fire effects monitoring and inventory system. Gen. Tech. Rep. RMRS-GTR-164. Fort Collins, CO: U.S. Department of Agriculture, Forest Service, Rocky Mountain Research Station

Mackenzie, W.H., & Meidinger, D. (2018). The Biogeoclimatic Ecosystem Classification Approach: an ecological framework for vegetation classification. *Phytocoenologia*, 48(2), 203-213.

Maltamo, M., Eerikäinen, K., Packalén, P., Hyyppä, J. (2006). Estimation of stem volume using laser scanning-based canopy height metrics. *Forestry: An International Journal of Forest Research*, 79(2), 217–229.

Maltamo, M., Bollandsås, O. M., Vauhkonen, J., Breidenbach, J., Gobakken, T., & Næsset, E. (2010). Comparing different methods for prediction of mean crown height in Norway spruce stands using airborne laser scanner data, *Forestry: An International Journal of Forest Research*, 83 (3), 257–268.

Martinuzzi, S., Vierling, L.A, Gould, W.A., Falkowski, M.J., Evans, J.S., Hudak, A.T. & Vierling, K. (2009). Mapping snags and understory shrubs for a LiDAR-based assessment of wildlife habitat suitability. *Remote Sensing of Environment*, 113, 2533-2546.

Matasci, G., Hermosilla, T., Wulder, M.A., White, J.C., Coops, N.C., Hobart, G.W. & Zald, H.S.J. (2018). Large-area mapping of Canadian boreal forest cover, height, biomass and other structural attributes using Landsat composites and lidar plots. *Remote Sensing of Environment*, 209, 90-106.

McComb, W. (2009). Ecology of coarse woody debris and its role as habitat for mammals. In W. McComb, Mammal Community Dynamics (pp. 374-404). Cambridge University Press.

Mehtätalo, L., Miguel, S., &. Gregoire T.G. (2015). Modeling height-diameter curves for prediction**.** *Canadian Journal of Forest Research*, 45 (7), 826-837.

Meidinger, D., and Pojar, J. (1991), Ecosystems of British Columbia. Special Report Series 6, Research Branch, B.C. Ministry of Forests, Victoria, Canada.

Miller, J.D., Danzer, S.R., Watts, J.M., Stone, S., &. Yool, S.R. (2003). Cluster analysis of structural stage classes to map wildland fuels in a Madrean ecosystem. *Journal of Environmental Management*, 68, 239-252.

Monleon, V., Gitelman, A., & Gray, A. (2002). Multi-scale Relationships Between Coarse Woody Debris and Presence/Absence of Western Hemlock in the Oregon Coast Range. *Springer*, New York, NY.

Morsdorf, F., Mårell, A., Koetz, B., Cassagne, N., Pimont, F., Rigolot, E., & Allgöwer, B. (2010). Discrimination of vegetation strata in a multi-layered Mediterranean forest ecosystem using height and intensity information derived from airborne laser scanning. *Remote Sensing of Environment*, 114(7), 1403-1415.

Mücke, W., Hollaus, M., Pfeifer, N., Schroiff, A., & Deák, B. (2013). Comparison of discrete and full-waveform ALS for dead wood detection. *ISPRS Annals of the Photogrammetry, Remote Sensing and Spatial Information Sciences*, 2, 199-204.

Mutlu, M., Popescu, S.C., Stripling, C & Spencer, T. (2008). Mapping surface fuel models using lidar and multispectral data fusion for fire behavior. *Remote Sensing of Environment*, 112(1), 274-285.

Muscolo A., Bagnato, S., Sidari, M., & Mercurio, R. (2014). A review of the roles of forest canopy gaps. *Journal of Forestry Research*, 25(4), 725–736.

Naesset, E and Tveite, B. (1999). Stand Volume Functions for Picea abies in Eastern, Central and Northern Norway. *Scandinavian Journal of Forest Research*, 14(2), 164 -174.

Naesset, E. (2002). Predicting forest stand characteristics with airborne scanning laser using a practical two-stage procedure and field data. *Remote Sensing of the Environment,* 80, 88-99.

Natural Resources Canada. (2018). The State of Canada's Forests. Annual Report 2018, Canadian Forest Service, Ottawa.

Nijland, W. Coops, N.C., Neilson, S.E., Wulder, M.A., & Steinhouse, G. (2014). Fine-Spatial Scale Predictions of Understory Species Using Climate and LiDAR-Derived Terrain and Canopy Metrics. *Journal of Applied Remote Sensing*, 8(1), 16.

Nijland, W., Coops, N.C, Nielsen, S.E. & Stenhouse, G. (2015). Integrating optical satellite data and airborne laser scanning in habitat classification for wildlife management. *International Journal of Applied Earth Observation and Geoinformation*, 38, 242-250.

Nilsson, M. & Wardle, D.A. (2005). Understory vegetation as a forest ecosystem driver: evidence from the northern Swedish boreal forest. *Frontiers in Ecology,* 3(8), 421-428.

Nunery, J., & Keeton, W. S. (2010). Forest carbon storage in the northeastern United States: net effects of harvesting frequency, post-harvest retention, and wood products. *Forest Ecology and Management*, 259, 1363–1375.

Nystrom (Firm). (2003). The Nystrom atlas of Canada and the world. Nystrom.

Nyström, M., Holmgren, J., Fransson, J., & Olsson, H. (2014). Detection of windthrown trees using airborne laser scanning. International Journal of Applied Earth *Observation and Geoinformation*, 30(1), 21-29.

Pan, Y., et al. (2011). A large and persistent carbon sink in the world's forests. *Science*, 333, 988–993.

Parker, G. G., & Russ, E. M. (2004). The canopy surface and stand development assessing forest canopy structure and complexity with near-surface altimetry. *Forest Ecology and Management*, 189, 307-315.

Pesonen, A., Maltamo, M., Eerikäinen, K., & Packalèn, P. (2008). Airborne laser scanning-based prediction of coarse woody debris volumes in a conservation area. *Forest Ecology and Management*, 255(8-9), 3288-3296.

Peterson, G. Allen, C.R. & Holling, C.S. (1998). Ecological Resilince, Biodiversity and Scale. *Ecosystems*, 1(1), 6-18.

Peterson, G. (2002). Contagious disturbance, ecological memory, and the emergence of landscape pattern. *Ecosystems*, 5(4), 329-338.

Pflugmacher, D., Cohen, W., & Kennedy, R. (2012). Using Landsat-derived disturbance history (1972-2010) to predict current forest structure. *Remote Sensing of Environment*, 122, 146-165.

Province of British Columbia. (2015). Field manual for describing terrestrial ecosystems. B.C. Ministry of Environment, Lands and Parks and B.C. Ministry of Forests, Victoria, B.C. Land Management Handbook. 25.

Pyke, D. A. & Zamora, B.A. (1982). Relationships between overstory structure and understory production in the grand fir/ myrtle boxwood habitat type of northcentral Idaho. *Journal of Range Management*, 35(6), 769-773.

R Core Team (2018) R: A Language and Environment for Statistical Computing. R Foundation for Statistical Computing, Vienna.

Raber, G., Jensen, J., Schlll, S., & Schuckman, K. (2002). Creation of Digital Terrain Models Using an Adaptive Lidar Vegetation Point Removal Process. *Photogrammetric Engineering and Remote Sensing*, 68(12), 1307 – 1315.

Reutebuch, S.E., McGaughey, R.J, Andersen, H., & Carson, W.W. (2003). Accuracy of a high-resolution lidar terrain model under a conifer forest canopy. *Canadian Journal of Remote Sensing*, 29, 527-535.

Riegel, G., Miller, R., & Krueger, W. (1992). Competition for Resources Between Understory Vegetation and Overstory Pinus Ponderosa in Northeastern Oregon. *Ecological Applications*, 2(1), 71-85.

Rogers, P. (2002). Using Forest Health Monitoring to assess aspen forest cover change in the southern Rockies ecoregion. *Forest Ecology and Management*, 155, 233-236.

Rollins, M.G., Keane, R.E., & Parsons, R.A. (2004). Mapping fuels and fire regimes using remote sensing, ecosystem simulation, and gradient modeling. *Ecological Applications*, 14, 75–95.

Rothermel, R. C. (1991). Predicting behavior and size of crown fires in the Northern Rocky Mountains. Res. Pap. INT-438. Ogden, UT: U.S. Department of Agriculture, Forest Service, Intermountain Forest and Range Experiment Station. 46 p.

Roussel, J.R., Auty, D. (2020) lidR: Airborne LiDAR Data Manipulation and Visualization for Forestry Applications. R package. Available online: https://github.com/Jean-Romain/lidR

Sahlin, E. & Ranius, T. (2009). Habitat availability in forests and clearcuts for saproxylic beetles associated with aspen. *Biodiversity and Conservation*, 18, 621-638. 10.1007/s10531-008-9528-8.

Schenk, T. (2001). Fusion of LIDAR data and aerial imagery for a more complete surface description. *International archives of the photogrammetry, remote sensing and spatial information sciences*, 24(3), 310.

Schoennagel, T., Balch, J.K., Brenkert-Smith, H., Dennison, P.E., Harvey, B.J., Krawchuk, M.A., Mietkiewicz, N., Morgan, P., Moritz, M.A., Rasker, R.,Turner, M.G., & Whitlock, C. (2017). Adapt to more wildfire in western North American forests as climate changes. *PNAS*, 114(18), 4582-4590.

Schmid, A., Vogel, C., Liebman, E., Curtis, P., & Gough, C. (2016). Coarse woody debris and the carbon balance of a moderately disturbed forest. *Forest Ecology and Management,* 361, 38-45.

Schulze, E., Wirth, C., & Heimann, M. (2000). Managing forests after Kyoto. *Science*, 289(5487), 2058-2059.

Scott, J.H., & Reinhardt, E.D. (2001). Assessing crown fire potential by linking models of surface and crown fire behavior. USDA Forest Service Research Paper RMRS-RP-29.

Seielstad, C.A., & Queen, L.P. (2003). Using airborne laser altimetry to determine fuel models for estimating fire behavior. The Journal of Forestry, 101(4), 10-15.

Shendryk, I., Broich, M., Tulbure, M., McGrath, A., Keith, D., & Alexandrov, S. (2016). Mapping individual tree health using full-waveform airborne laser scans and imaging spectroscopy: A case study for a floodplain eucalypt forest. *Remote Sensing of Environment*, 187, 202-217.

Shifley, S., He, H., Lischke, H., Wang, W., Jin, W., Gustafson, E., Yang, J. (2017). The past and future of modeling forest dynamics: from growth and yield curves to forest landscape models. *Landscape Ecology*, 32(7), 1307-1325.

Shugart, H. (1984). A Theory Of Forest Dynamics: The ecological implications of forest succession. The Blackburn Press.

Smallman, T., Exbrayat, J.-F., Mencuccini, M., Bloom, A., & Williams, M. (2017). Assimilation of repeated woody biomass observations constrains decadal ecosystem carbon cycle

uncertainty in aggrading forests. *Journal of Geophysical Research: Biogeosciences*, 122(3), 528-545.

Spies, T.A. (1998). Forest structure: a key to the ecosystem. *Northwest Science*, 72, 34-39.

Stone, M.G. (1998). Forest-type mapping by photo-interpretation: a multi-purpose base for Tasmania's forest management. *Tasforests*, 10, pp. 15-32

Sturtevant, B., Bissonette, J., Long, J., & Roberts, D. (1997). Coarse Woody Debris as a Function of Age, Stand Structure, and Disturbance in Boreal Newfoundland. *Ecological Applications*, 7(2), 702.

Stutz, K., & Lang, F. (2017). Potentials and Unknowns in Managing Coarse Woody Debris for Soil Functioning. *Forests*, 8(2), 37.

Swanson, M., Franklin, J., Beschta, R., Crisafulli, C., DellaSala, D., Hutto, R., Swanson, F. (2011). The forgotten stage of forest succession: Early-successional ecosystems on forest sites. *Frontiers in Ecology and the Environment*, 9(2), 117-125.

Taboada, Á., Tárrega, R., Calvo, L., Marcos, E., Marcos, J., & Salgado, J. (2010). Plant and carabid beetle species diversity in relation to forest type and structural heterogeneity. *European Journal of Forest Research*, 129(1), 31-45.

Tanhuanpää, T., Kankare, V., Vastaranta, M., Saarinen, N., & Holopainen, M. (2015). Monitoring downed coarse woody debris through appearance of canopy gaps in urban boreal forests with bitemporal ALS data. *Urban Forestry and Urban Greening*, 14(4), 835-843.

Tompalski, P., Coops, N.C., White, J.C. & Wulder, M.A. (2015). Enriching ALS-Derived Area-Based Estimates of Volume through Tree-Level Downscaling. *Forests*, 6(8), 2608-2630.

Turner, M., Gardner, R., Dale, V., & O'Neill, R. (1989). Predicting the Spread of Disturbance across Heterogeneous Landscapes. *Oikos*, 55(1): 121-129.

van Aardt, J.A., Arthur, M., Sovkoplas, G., and Swetnam, T.L. (2011). LiDAR-based estimation of forest floor fuel loads using a novel distributional approach. In Proceedings of

SilviLaser 2011, 11th International Conference on LiDAR Applications for Assessing Forest Ecosystems, University of Tasmania, Australia, 16–20 October 2011. pp. 1–8.

van Ewijk, K. Y., Treitz, P. M., & Scott, N. A. (2011). Characterizing Forest Succession in Central Ontario using LAS-derived Indices. *Photogrammetric Engineering and Remote Sensing*, 77(3), 261-269.

Van Leeuwen, M., Coops, N., & Wulder, M. (2010). Canopy surface reconstruction from a LiDAR point cloud using Hough transform. *Remote Sensing Letters*, 1(3), 125-132.

Wang, T., Hamman, A. and Aitkin, S.N. (2007). ClimateBC v3.2: A program to generate climate normal, decade, annual, seasonal and monthly data for genecology and climate change studies in British Columbia. Available online (accessed October 27, 2008): http://www.genetics.forestry.ubc.ca/cfcg/climate-models.html

West, P.W. (2009). Tree and Forest Measurement, 2nd edition.

White, J.C., Wulder, M.A., Varhola, A., Vastaranta, M., Coops, N.C., Cook, B.D., Pitt, D. & Woods, M. (2013). A best practices guide for generating forest inventory attributes from airborne laser scanning data using an area-based approach. *Forestry Chronicles*, 89: 722-723.

White, J.C., Tompalski, P., Vastaranta, M., Wulder, M.A., Saarinen, N., Stepper, C., & Coops, N.C. 2017. A model development and application guide for generating an enhanced forest inventory using airborne laser scanning data and an area-based approach. CWFC Information Report FI-X-018, Canadian Forest Service, Pacific Forestry Centre: Victoria, BC, Canada. Available from: http://cfs.nrcan.gc.ca/pubwarehouse/pdfs/38945.pdf

White, J.C., Tompalski, P., Coops, N., & Wulder, M. (2018). Comparison of airborne laser scanning and digital stereo imagery for characterizing forest canopy gaps in coastal temperate rainforests. *Remote Sensing of Environment*, 208, 1-14.

Whitehead, D., 1978. The Estimation of Foliage Area from Sapwood Basal Area in Scots Pine. *Forestry*, 51 (2) (1978), pp. 137-149

Whitman, E., Rapaport, E., & Sherren, K. (2013). Modeling fire susceptibility to delineate wildland-urban interface for municipal-scale fire risk management. *Environmental Management*, 52(6), 1427-1439.

Wilbert, C., Buskirk, S., & Gerow, K. (2000). Effects of weather and snow on habitat selection by American martens (*Martes americana*). *Canadian Journal of Zoology*, 78(10), 1691-1696.

Wilkes, P., Jones, S., Suarez, L., Haywood, A., Woodgate, W., Soto-Berelov, M., Skidmore, A. (2015). Understanding the effects of ALS pulse density for metric retrieval across diverse forest types. *Photogrammetric Engineering and Remote Sensing*, 81(8), 625-635.

Wing, B.M., Ritchie, M.W., Boston, K., Cohen, W.B., Gitelman, A. & Olsen, M.J. (2012). Prediction of understory vegetation cover with airborne lidar in an interior ponderosa pine forest. Remote Sensing of Environment 124: 730-741.

Wing, B., Ritchie, M., Boston, K., Cohen, W., & Olsen, M. (2015). Individual snag detection using neighborhood attribute filtered airborne lidar data. *Remote Sensing of Environment*, 163, 165-179.

Woodall, C.W., Heath, L.S., & Smith, J.E. (2008) National inventories of down and dead woody material forest carbon stocks in the United States: Challenges and opportunities. *Forest Ecology and Management*, 256(3), 221-228.

Woodall, C.W., & Liknes, G.C. (2008) Relationships between forest fine and coarse woody debris carbon stocks across latitudinal gradients in the United States as an indicator of climate change effects. *Ecological Indicators*, 8, 686-690.

Wulder, M.A., (1998). Optical remote-sensing techniques for the assessment of forest inventory and biophysical parameters. *Progress in Physical Geography: Earth and Environment*, 22(4), 449-476.

Wulder, M.A., Kurz, W., & Gillis, M. (2004). National level forest monitoring and modelling in Canada. Progress in Planning, 61(4), 365-381.

Xiong, L., Wang, G., Bao, Y., Zhou, X., Sun, X., & Zhao, R. (2018). Detectability of Repeated Airborne Laser Scanning for Mountain Landslide Monitoring. *Geosciences*, 8(12), 469.

Yamamoto, S. (2000). Forest Gap Dynamics and Tree Regeneration. *Journal of Forest Research*, 5(4), 233-239.

Zhang, W., Qi, J., Wan, P., Wang, H., Xie, D., Wang, X., & Yan, G. (2016). An Easy-to-Use Airborne LiDAR Data Filtering Method Based on Cloth Simulation. *Remote Sensing*, 8(6), 501.

Zhang, Z., Lin, C., & She, G. (2017). Estimating Forest Structural Parameters Using Canopy Metrics Derived from Airborne LiDAR Data in Subtropical Forests. *Remote Sensing*, 9(9), 940.

Zhou, L., Dai, L.-m., Gu, H.-y., & Zhong, L. (2007). Review on the decomposition and influence factors of coarse woody debris in forest ecosystem. *Journal of Forestry Research*, 18(1), 48-54.